A THESIS

FOR THE DEGREE OF DOCTOR OF PHILOSOPHY

Acid-processing and fermentation of *Hizikia fusiforme* and bioactivities of fucoidan from the processed *H. fusiforme*

Yong Ri Cui

Department of Marine Life Sciences

GRADUATE SCHOOL

JEJU NATIONAL UNIVERSITY

February, 2020

Acid-processing and fermentation of *Hizikia fusiforme* and bioactivities of fucoidan from the processed *H. fusiforme*

Yong Ri Cui

(Supervised by Professor You-Jin Jeon)

A thesis submitted in partial fulfilment of the requirement for the degree of

DOCTOR OF PHILOSOPHY

February 2020

The thesis has been examined and approved by

.....

Thesis director, Gi-Young Kim (PhD), Professor of Marine Life Sciences, Jeju National University

.....

Choon Bok Song (PhD), Professor of Marine Life Sciences, Jeju National University

.....

BoMi Ryu (PhD), Marine Science Institute, Jeju National University

.....

Jae-Young Oh(PhD), Department of Marine Life Sciences, Jeju National University

.....

You-Jin Jeon (PhD), Professor of Marine Life Sciences, Jeju National University

02/2020
Date

Department of Marine Life Sciences

Graduate School

Jeju National University

Republic of Korea

CONTENT

SUMMARY

Hizikia fusiforme is the most popular edible seaweed in Asian countries such as Korea, China, and Japan. *H. fusiforme* is a rich and potential natural resource could be used as an ingredient in functional food and medicine, industries. Many reports support that *H. fusiforme* contains various natural bioactive compounds and possess the potential to develop functional food and medicine. However, the arsenic (As) in *H. Fusiforme* is a serious threat to food safety and it restricts the on the application of *H. Fusiforme*. Therefore, in the present study, we remove of the arsenic from *H. fusiforme* by acid-processing and fermentation, and isolation of bioactive compound from the fermented *H. fusiforme* as well as evaluation of its bioactivities.

In the present study, *H. fusiforme* was processed by citric acid (CA) and hydrochloric acid (HA). The results indicated that CA-processed *H. fusiforme* contains a low As amount. In addition, the optimal CA process condition has been investigated by response surface methodology experiment. Finally, the CA-processing condition has been decided as washing suing the water contain 0.4% of CA for 120 min at 60℃, and 97.11% As of *H. fusiforme* had been removed after processing at the optimal condition.

In order to further remove of the As from *H. fusiforme*, the CA-processed *H. fusiforme* was fermented by different of probiotics. The results indicated that the *H. fusiforme* fermented by *Lactobacillus rhamnosus* possesses the lowest As content and highest reducing capacity. Therefore, *Lactobacillus rhamnosus* was selected as the strain to fermentation of CA-processed *H. fusiforme*. In addition, the chemical composition and bioactivities of non-fermented and fermented *H. fusiforme* were investigated. The results displayed that the

bioactivities of *H. fusiforme* were increased after fermentation and the main composition of fermented *H. fusiforme* is polysaccharides.

The crude polysaccharides (HFF-PS) of fermented *H. fusiforme* (HFF) were separated by ethanol precipitation. HFF-PS contains high amount polysaccharides (60.63%) and sulfated content (17.18%), as well as possesses strong antioxidant and anti-inflammatory activity. Thus, it has been further purified. After purification, an active fraction (HFF-PS-F5) was separated from the crude polysaccharides (HFF-PS) from fermented *H. fusiforme*. HFF-PS-F5 contains 91.68% sulfated polysaccharides, which comprise fucose (53.84%), galactose (19.08%), glucose (2.22%), and mannose (24.86%). In addition, the characteristics of HFF-PS-F5 had been determined by Fourier-transform infrared (FT-IR) and HPGPC. The results indicated that HFF-PS-F5 is the fucoidan with an average molecular weight as 213.33 kDa.

Protective effect of the fucoidan (HFF-PS-F5) isolated from HFF-PS against hydrogen peroxide (H_2O_2)-induced oxidative stress *in vitro* in Vero cells and *in vivo* in zebrafish had been investigated. HFF-PS-F5 significantly reduced cytotoxicity induced by H_2O_2 in Vero cells. In addition, HFF-PS-F5 reduced intracellular ROS level and apoptosis body formation induced by H_2O_2. The Western blot results demonstrate that HFF-PS-F5 against oxidative stress by improving the expression of endogenous antioxidant enzymes including catalase and superoxidase dismutase (SOD) via regulating Nrf2 pathways. In addition, HFF-PS-F5 has strongly protective against H_2O_2-stimulated oxidative stress *in vivo* zebrafish that demonstrated in improving survival rate, decreasing heart beating rate, and reducing ROS generation, cell death and lipid peroxidation. These results suggest that HFF-PS-F5 may use as a beneficial antioxidant ingredient in medical and cosmetic industries.

LIST OF TABLE

LIST OF FIGURE

conducted in triplicate, and the data are expressed as the mean ± SE. *$p < 0.05$, ** $p < 0.01$ as compared to the H_2O_2-treated group and $^{\#\#}p < 0.01$ as compared to the control group.

Fig. 26. The protective effect of HFF-PS-F5 during H_2O_2-induced cell death in zebrafish embryos. (A) Zebrafish embryo under fluorescence microscope; (B) the measured levels of cell death. Cell death levels were measured using Image J software. The experiments were conducted in triplicate, and the data are expressed as the mean ± SE. *$p < 0.05$, ** $p < 0.01$ as compared to the H_2O_2-treated group and $^{\#\#}p < 0.01$ as compared to the control group.

Fig. 27. The protective effect of HFF-PS-F5 during H_2O_2-induced lipid peroxidation in zebrafish embryos. (A) Zebrafish embryo under fluorescence microscope; (B) the measured levels of cell death. Cell death levels were measured using Image J software. The experiments were conducted in triplicate, and the data are expressed as the mean ± SE. *$p < 0.05$, ** $p < 0.01$ as compared to the H_2O_2-treated group and $^{\#\#}p < 0.01$ as compared to the control group.

Fig. 28. The effect of HFF-PS-F5 on LPS-induced NO generation and cytotoxicity in RAW 264.7 macrophages. (A) NO production in LPS-induced RAW 264.7 macrophages and (B) Cell viability in LPS-induced RAW 264.7 macrophages. The experiments were conducted in triplicate, and the data are expressed as the mean ± SE. *$p < 0.05$, ** $p < 0.01$ as compared to the LPS-treated group and $^{\#\#}p < 0.01$ as compared to the control group.

Fig. 29. The inhibitory effect of HFF-PS-F5 upon the production of PGE_2 (A) , TNF-α (B), IL-1β (C) , and IL-6 (D) in LPS-stimulated RAW 264.7 macrophages. The experiments were conducted in triplicate, and the data are expressed as the mean ±SE. ** $p < 0.01$ as compared to the LPS-treated group and $^{\#\#}p < 0.01$ as compared to the control group.

Fig. 30. The inhibitory effect of HFF-PS-F5 on the expression of iNOS and COX-2 proteins in RAW 264.7 macrophages stimulated with LPS. The relative amounts of iNOS and COX-2 levels were compared with β-actin. The experiments were conducted in triplicate, and the data are expressed as the mean ± SE. *$p < 0.05$, ** $p < 0.01$ as compared to the LPS-treated group and $^{\#\#}p < 0.01$ as compared to the control group.

Fig. 31. The inhibitory effect of HFF-PS-F5 on NF-κB activation in RAW 264.7 macrophages stimulated with LPS. (A) The cytosol IκBα and p-IκBα level; (B) the nuclear p50 and p65 NF-κB level. The relative amounts of IκBα and p-IκBα levels were compared with β-actin, and the relative amounts of p50 and p65 NF-κB levels were compared with nucleolin. The experiments were conducted in triplicate, and the data are expressed as the mean ± SE. ** $p < 0.01$ as compared to the LPS-treated group and $^{\#\#}p < 0.01$ as compared to the control group.

Fig. 32. The survival rate and heart-beating rate of zebrafish after pretreatment with HFF-PS-F5 and/or treatment with LPS. (A) Survival rate; (B) heart-beating rate. The experiments were conducted in triplicate, and the data are expressed as the mean ± SE. *$p < 0.05$, ** $p < 0.01$ as compared to the LPS-treated group and $^{\#\#}p < 0.01$ as compared to the control group.

Fig. 33. The protective effect of HFF-PS-F5 during LPS-induced ROS production in zebrafish embryos. (A) Zebrafish embryo under fluorescence microscope; (B) the levels of ROS generation. ROS levels were measured using Image J software. The experiments were conducted in triplicate, and the data are expressed as the mean ± SE. *$p < 0.05$, ** $p < 0.01$ as compared to the LPS-treated group and $^{\#\#}p < 0.01$ as compared to the control group.

Fig. 34. The protective effect of HFF-PS-F5 during LPS-induced cell death in zebrafish embryos. (A) Zebrafish embryo under fluorescence microscope; (B) the measured levels of cell death. Cell death levels were measured using Image J software. The experiments were conducted in triplicate, and the data are expressed as the mean ± SE. ** $p < 0.01$ as compared to the LPS-treated group and $^{\#\#}p < 0.01$ as compared to the control group.

Fig. 35. The effect of HFF-PS-F5 during LPS-induced NO production in zebrafish embryos. (A) Zebrafish embryo under fluorescence microscope; (B) the measured levels of cell death. NO production levels were measured using Image J software. The experiments were conducted in triplicate, and the data are expressed as the mean ± SE. ** $p < 0.01$ as compared to the LPS-treated group and $^{\#\#}p < 0.01$ as compared to the control group.

INTRODUCTION

Oxidative stress is relate to the development of cancer, inflammation, diabetes, obesity, Parkinson's disease, Alzheimer's disease, aging, and other diseases [1-5]. It reflects an imbalance between reactive oxygen species (ROS) generation and scavenging. ROS including hydrogen peroxide (H_2O_2) and free radicals such as superoxide anion radical ($O_2•^-$) and hydroxyl radical (HO•), which are naturally generated during normal cellular metabolic processes [6]. Generally, the amount of ROS generated by normal metabolic can be scavenged by the cellular endogenous antioxidant system [7] . However, the excessive environmental stresses such as ultraviolet irradiation, fine dust particles, and chemicals can cause an abnormal ROS production that leads to several diseases [8]. Therefore, the antioxidant component that possesses strong ROS scavenging effect and non-toxicity may an ideal candidate to develop a therapeutic agent against diseases caused by oxidative stress.

Inflammation is a complex biological response of the body to harmful stimuli. It is a protective response involving immune cells such as macrophage, blood vessels, and molecular mediators such as nitric oxide (NO), pro-inflammatory cytokines such as tumor necrosis factor alpha (TNF-α), interleukin-1 beta (IL-1β), and interleukin-6 (IL-6), prostaglandins, and other molecules [9]. However, uncontrolled or chronic inflammation may cause chronic inflammation-related diseases such as rheumatoid arthritis and cardiovascular diseases [10-12]. Macrophages play an important role during the development of inflammatory diseases caused by overproduction of pro-inflammatory cytokines and other inflammatory molecules [13]. Therefore, to inhibit the production of these inflammation-related molecules is a possible strategy to against the inflammatory diseases.

The ocean is covering approximately 71% of the Earth's surface. The ocean contains 97% of Earth's water and 90% of the Earth's biosphere. The ocean is abundant with a complex diversity of marine organisms, which including marine animals such as fish and shellfish, marine microorganisms such as bacteria and fungi, and marine plants such as algae and sea grasses. The marine organisms offer a rich source of natural products, such as phenolic compounds, lipids, proteins, minerals, polysaccharides, and essential vitamins [14]. These natural compounds possess various bioactivities including anti-inflammatory, antioxidant, anti-cancer, anti-microbial, anti-irradiation, anti-diabetes, anti-hypertension, and anti-obesity activities [15-22]. Sun et al. (2009) had isolated antioxidant polysaccharides from marine fungus *Penicillium* sp. F23-2 [23]. Ko et al. (2012) had isolation and characterization the angiotensin I-converting enzyme inhibitory peptide from *Styela clava* [24]. Kang et al. (2016) had investigated anti-obesity effects of seaweeds of Jeju Island 3T3-L1 preadipocytes and obese mice [22].

Algae can be classified into two subtypes that microalgae and macroalgae. Microalgae are unicellular species and the sizes of microalgae can range from micrometers to hundred micrometers. Microalgae exist individually, or in groups or chains. Macroalgae are macroscopic and multicellular. Marine macroalgae are referring as seaweed and it includes red, green, and brown seaweed. Seaweeds contain a large mass of nutrient contents such as minerals, vitamins, carbohydrates, proteins, fatty acids, and amino acids. It is also rich in natural compounds including polysaccharides, proteins, sterols, polyphenols, fatty acids, amino acids, alkaloids, and pigments, as well as possesses wide range a broad spectrum of bioactivity such as anti-microbial, antioxidant, anti-cancer, anti-coagulation, anti-aging, anti-inflammation, anti-irradiation, anti-hypertension, anti-obesity, and anti-diabetes properties [25-35]. Wijesinghe et al. (2011) had purified a sulfated polysaccharide from

Ecklonia cava and evaluated its anti-coagulative activity [36]. Heo et al. had isolated a pigment, fucoxanthin from *Sargassum siliquastrum* and investigated the protective effect of fucoxanthin against ultraviolet B (UVB)-induced cell damage [37]. Kang et al. (2012) had isolated a polyphenol, dieckol from *Ecklonia cava* and investigated the hepatoprotective effect of dieckol [38]. Souza et al. (2009) had isolated and identified a bisindole alkaloid, caulerpin from *Genes gaulerpa* and evaluated the anti-inflammatory and antinociceptive effects of caulerpin in mice [35]. In addition, Fernando et al. (2018) had isolated alginic acid from *Sargassum horneri* and evaluated its anti-inflammatory effect [32]. Wang et al. (2019) had investigated the melanogenesis inhibition effects of a mixture of seaweed extract and glycosaminoglycans from sea squirts in α-MSH-stimulated B16F10 melanoma cells [39].

Edible seaweed or sea vegetable is the seaweeds, which can be directly eaten or used as a material for preparing food. Consumption of seaweeds as a food or medicine material has a long history, especially in Asian countries [25, 40]. Recent decade reports suggest that edible seaweeds are benefiting for human's health because they are rich in nutrients and various bioactive compounds, which could prevent, improve, or against above diseases [41-44]. Nowadays, there are many species of edible seaweeds had been large-scale cultured such as *Saccharina jiaponica*, *Hizikia fusiforme*, *Undaria pinnatifida*, and *Porphyra yezoensis*, as well the edible seaweed had used for a wide range of food, pharmacy, and cosmetic industries [45-49].

Seaweeds contain various bioactive compounds, especially polysaccharides. Algal polysaccharides generally comprise carrageenan, fucoidan, and alginate. Normally, algal polysaccharides have unique physicochemical properties and possess potent bioactivities, such as antioxidant, anti-inflammatory, anticancer, anti-coagulant, radioprotective effect, immune activation, and renoprotective effects [12-19]. Lee et al. had reported antioxidant

activity of polysaccharide from *Pyropia yezoensis* [20]. Lee et al. had reported anti-inflammatory effect of fucoidan from *Ecklonia cava* [21]. In addition, Ahn et al. had reported immune system activation and modulation effects and anticancer activity of the sulfated polysaccharide from *Ecklonia cava* [22, 23]. Recently, to finding the functional polysaccharide from seaweed and developing it as a therapeutic agent to overcoming difficult miscellaneous had taken more and more attention.

Sulfated polysaccharides isolated from marine algae possess various health benefits such as antioxidant, anti-cancer, anti-inflammation, anti-melanogenesis, anti-allergic, and anti-coagulant activities [50]. In the past decades, various sulfated polysaccharides isolated from marine algae with its nutriceutical, pharmaceutical, and cosmeceutical potential had been reported [47, 51-53]. Hu et al. had isolated a sulfated polysaccharide from *Laminaria japonica* and investigated its effect on skin aging in mice [54]. Hwang et al. had reported the anti-inflammatory effect of the sulfated polysaccharide extract of *Sargassum hemiphyllum* [55]. In addition, Pratoomthai et al. had investigated the anti-melanogenesis effect of sulfated galactans isolated from the red alga, *Gracilaria fisheri* [56]. Recently, investigated the bioactivities of algal sulfated polysaccharides and applied them as an ingredient in pharmaceutical, nutriceutical, and cosmeceutical industries has taken more attention.

Hizikia fusiforme (*H. fusiforme*) is an edible brown seaweed and mainly grows in the northwest Pacific. *H. fusiforme* is one of the most of popular seaweed consumed as food in Asian countries, especially in Korea, China, and Japan. *H. fusiforme* had used as herb medicine for a long history [57]. It contents various bioactive compounds, especially polysaccharides. Polysaccharides from *H. fusiforme* possess extensive and potent bioactivities, including immune-modulating, anti-coagulant, and against ethanol-induced toxicity effects [24-26]. Wang et al. (2018 and 2019) had isolated and characterized sulfated

polysaccharides from the enzyme-assisted extract from *H. fusiforme*, as well as investigated the antioxidant, anti-inflammatory, anti-melanogenesis, UVB protective, and anti-wrinkle effects [47, 58-60]. The results suggested that the sulfated isolated form *H. fusiforme* possesses potent health benefits, which displayed in reducing hydrogen peroxide (H_2O_2)-induced oxidative stress in monkey kidney fibroblast cells (Vero cells) and in zebrafish; remarkable attenuating lipopolysaccharide (LPS)-induced inflammation in RAW 264.7 macrophages; inhibiting alpha-melanocyte stimulating hormone (α-MSH)-stimulated melanogenesis in B16F10 melanoma cells; protecting against UVB-induced photo-damage in keratinocytes (HaCaT cells) and in zebrafish; protecting UVB-induced skin wrinkling in human dermal fibroblasts (HDF cells).

The objectives of the present study are as follow: remove of the arsenic from *H. fusiforme* by acid-processing; fermentation of acid-processed *H. fusiforme*; isolation, purification, and characterization of polysaccharides from fermented *H. fusiforme*; investigation of bioactivities of fucoidan isolated from fermented *H. fusiforme* in *in vitro* and *in vivo* models.

Part I.

Remove of the arsenic from *Hizikia fusiforme* by acid-processing

Part I.

Remove of the arsenic from *Hizikia fusiforme* by acid-processing

Abstract

H. fusiforme has a strong ability to enrich arsenic (As) in seawater, and excessive intake of arsenic has serious harm to human body, so in the development of *H. fusiforme* products, it needs to remove of arsenic. In the present study, we process the *H. fusiforme* by citric acid (CA) and hydrochloric acid (HA) washing. The results indicated that CA-washed *H. fusiforme* contain lower as compared to HA-washed and non-washed *H. fusiforme*. In addition, the optimal CA process condition has been investigated by response surface methodology experiment. Finally, the CA-processing condition has been decided as washing suing the water contain 0.4% of CA for 120 min at 60℃, and 97.11% As of *H. fusiforme* had been removed after processing at the optimal condition.

1. Materials and methods

1.1. Reagents and chemicals

H. fusiforme was collected from Wenzhou, China, at May 2018. Citric acid (CA), hydrochloric acid (HA), thiourea, ascorbic acid, and standard arsenic (As) solution (0.1 g/L) were purchased from Sigma Co. (St. Louis, MO, USA). All other chemicals and reagents were analytical grade.

1.2. Processing *H. fusiforme* by acid washing

The acid-process conditions of *H. fusiforme* were summarized in Table 1. The *H. fusiforme* were processed by the method as follow:

Group 1: Non-processed *H. fusiforme*, grind to powder;

Group 2: *H. fusiforme*, add 15-folds weight of water, heat preservation and stir for 15 min at 90℃, dry at 105℃ for 5 h and grind the powder;

Group 3: *H. fusiforme*, add 40-folds weight of water, 0.6% of CA (W/V), preservation and stir for 120 min at 50℃, dry at 105℃ for 5 h and grind the powder;

Group 4: *H. fusiforme*, add 40-folds weight of water, 0.6% of HA (W/V), preservation and stir for 120 min at 50℃, dry at 105℃ for 5 h and grind the powder;

Group 5: Step one: *H. fusiforme*, add 15-folds weight of water, heat preservation and stir for 15 min at 90℃, remove the water;

Step two: *H. fusiforme* after processed by step one, add 20-folds weight of water, 0.6% of CA (W/V), preservation and stir for 120 min at 50℃, dry at 105℃ for 5 h and grind the powder;

Group 6: Step one: *H. fusiforme*, add 15-folds weight of water, heat preservation and stir for 15 min at 90℃, remove the water;

Step two: *H. fusiforme* after processed by step one, add 20-folds weight of water, 0.6% of HA (W/V), preservation and stir for 120 min at 50℃, dry at 105℃ for 5 h and grind the powder;

Table 1. Acid-process condition of *H. fusiforme.*

No.	Group	Hot water (HW)	Citric acid (CA)	Hydrochloric acid (HA)
1	Blank	N	N	N
2	HW	Y	N	N
3	CA	N	Y	N
4	HA	N	N	Y
5	HW+CA	Y	Y	N
6	HW+HA	Y	N	Y

Blank: Non-processed; Y: Yes; N: Not.

1.3. Measurement of As content of acid-processed *H. fusiforme*

The As content was determined by Hydride Generation-Atomic Fluorescence Spectrometer (HG-AFS) [31, 61-63]. Samples of 0.1g (up to 0.001g) were weighed into a 25mL colorimetric tube and mixed with 50% hydrochloric acid solution and sonication. The sample was fully extracted after 20 min, and then taken out for cooling and filtration. Taken 2 mL of sample solution and placed in 10 mL colorimetric tube, 1 mL of thiourea (5%) and ascorbic acid (5%) solution was added. The volume was fixed with deionized water and the solution was shaken and placed for 20 min to be tested. After preheating for 20~30min, the atomic fluorescence spectrometer started the measurement, followed by standard series measurement and sample measurement, and the reagent space ratio experiment.

1.4. Processing *H. fusiforme* by CA-washing with different conditions

In order to optimal the CA-processing condition, *H. fusiforme* was processed with CA at different conditions as follow:

Group 1(CA concentration): Step one: *H. fusiforme*, add 15-folds weight of water, heat preservation and stir for 15 min at 90℃, remove the water;

Step two: *H. fusiforme* after processed by step one, add 20-folds weight of water and added 0.2, 0.4, 0.6, 0.8, and 1.0% of CA (W/V), respectively. And then, preservation and stir for 120 min at 50℃, dry at 105℃ for 5 h and grind the powder;

Group 2 (processing time): Step one: *H. fusiforme*, add 15-folds weight of water, heat preservation and stir for 15 min at 90℃, remove the water;

Step two: *H. fusiforme* after processed by step one, add 20-folds weight of water, 0.6% of CA (W/V), preservation and stir for 80, 100, 120, 130, and 150 min at 50℃, respectively. And then dry at 105℃ for 5 h and grind the powder;

Group 3 (processing temperature): Step one: *H. fusiforme*, add 15-folds weight of water, heat preservation and stir for 15 min at 90℃, remove the water;

Step two: *H. fusiforme* after processed by step one, add 20-folds weight of water, 0.6% of CA (W/V), preservation and stir for 120 min at 30, 40, 50, 60, and 70℃, respectively. And then dry at 105℃ for 5 h and grind the powder.

1.5. Optimizing the CA-processing condition by response surface methodology (RSM)

RSM was used to optimize the CA-processing parameters of BBD with three factors at three levels based on single-factor experiments. CA concentration, processing time, and processing temperature (Table 2) were selected for the optimization of CA-processing. Using the Boxe-Behnken method, the whole design matrix was composed of 17 experiments in random order. The design of the experiments is given in Table 3 [64].

Table 2. RSM experimental factors and codes.

Code	Experimental factor		
	A: Concentration of CA (%)	**B**: Time (min)	**C**: Temperature (℃)
-1.000	0.2	100	50
0.000	0.4	120	60
1.000	0.6	140	70

2. Results and discussion

2.1. As content of *H. fusiforme* processed by different conditions

H. fusiforme was processed by different conditions and the As content of processed *H. fusiforme* was investigated. As shown in Fig. 1, the As content of non-processed *H. fusiforme* was 71.18 mg/kg, however, the As content of all processed *H. fusiforme* were significantly decreased compared to non-processed *H. fusiforme*. The *H. fusiforme* sequential processed by hot water and CA, which contains the lowest As content (9.09 mg/kg) in all of *H. fusiforme* samples. These results indicated that hot water and CA sequential processing is the best processing method for removing As from *H. fusiforme*.

2.2. As content of *H. fusiforme* processed by CA with different conditions

In order to optimal the CA-processing condition, *H. fusiforme* was processed with CA at different conditions and the As content of processed *H. fusiforme* was investigated. As Fig. 2 shows, the As contents of *H. fusiforme* processed by 0.2, 0.4, 0.6, 0.8, and 1.0% of CA at 50℃ for 120 min were 11.87, 10.72, 9.03, 9.04, and 9.09 mg/kg, respectively. The *H. fusiforme* sequential processed by hot water and 0.6% of CA, which contains the lowest As content (9.03 mg/kg) in all of processed *H. fusiforme* samples. These results indicated that 0.6% of CA is the best concentration for processing of *H. fusiforme*.As shown in Fig. 3, the As contents of *H. fusiforme* processed by 0.6% of CA at 50℃ for 80, 100, 120, 130, and 150 min were 11.91, 10.03, 8.33, 8.29, and 8.22 mg/kg, respectively. The *H. fusiforme* sequential processed by for 150 min, which contains the lowest As content (8.22 mg/kg) in all of processed *H. fusiforme* samples. In addition, the As content of *H. fusiforme* processed by 120, 130, and 150 min are not much change. Thus, that 120 min may the best processing time for processing of *H. fusiforme*.

Under the condition that the concentration of CA was 0.6% and the processing time was 120 min, the temperatures were changed to: 30, 40, 50, 60 and 70℃, to investigate the effect of temperature on the removal of As. The results are shown in Fig. 4. Within the range of 30℃ to 50℃, the removal amount of As decreases significantly with the increase of temperature. After 50℃, the removal of As reaches saturation, and the content of As basically remains unchanged with the change of temperature. According to these results, we can know that 50℃ may the best temperature for processing of *H. fusiforme*.

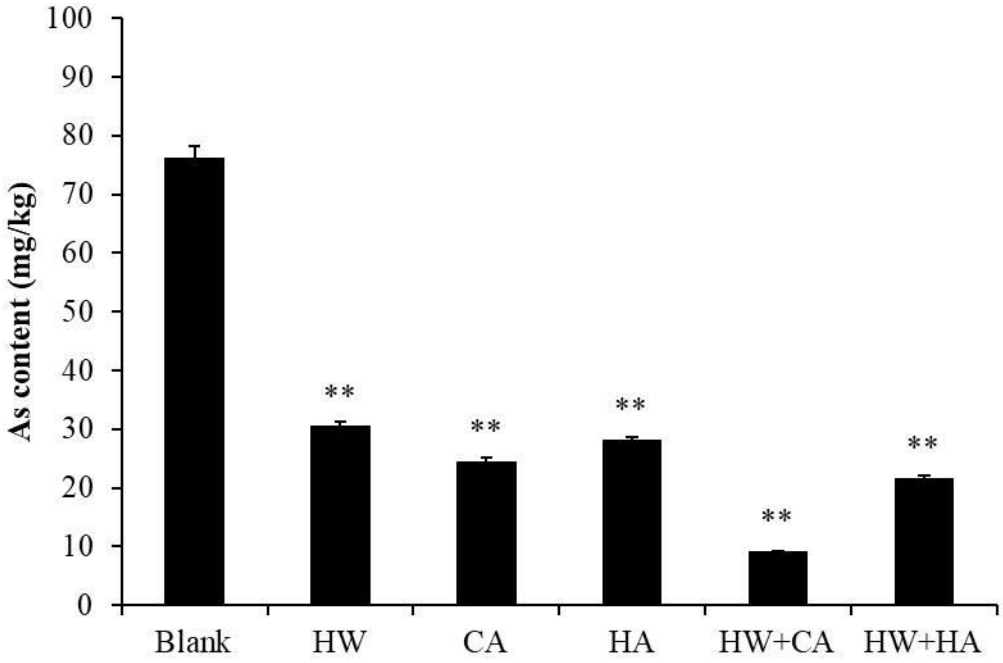

Fig. 1. As content of *H. fusiforme* after processing. ***p*<0.01 compared to blank group.

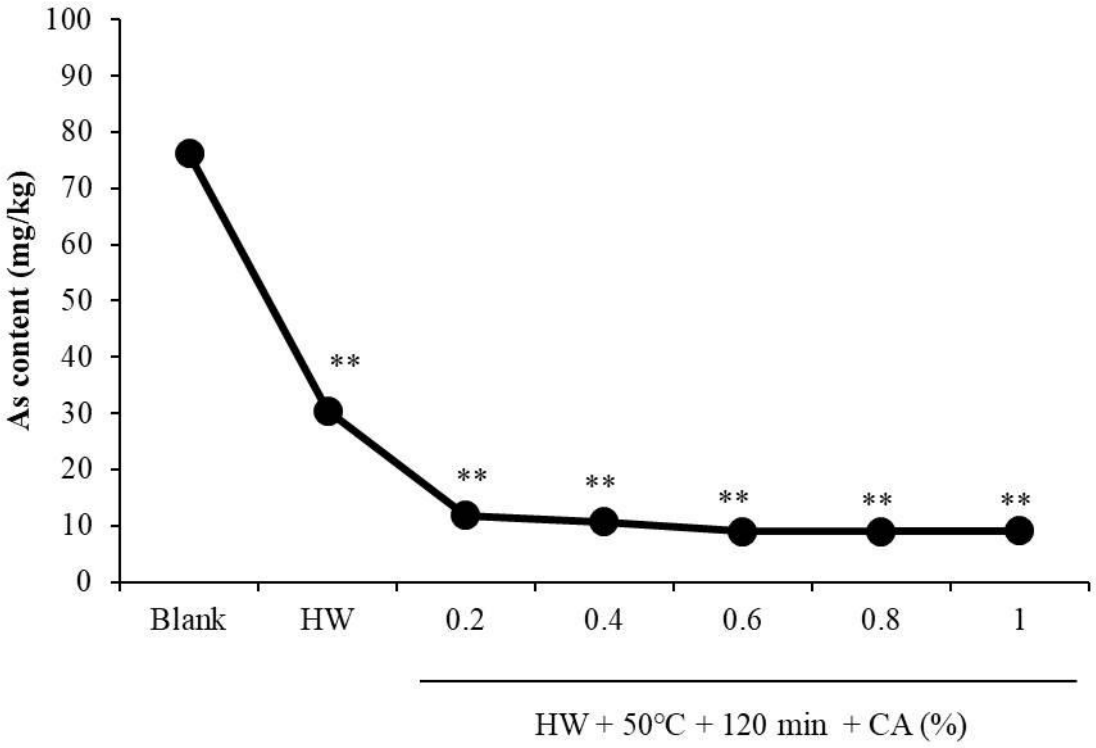

Fig. 2. As content of *H. fusiforme* after processing after processing by different concentrations of CA. ***p*<0.01 compared to blank group.

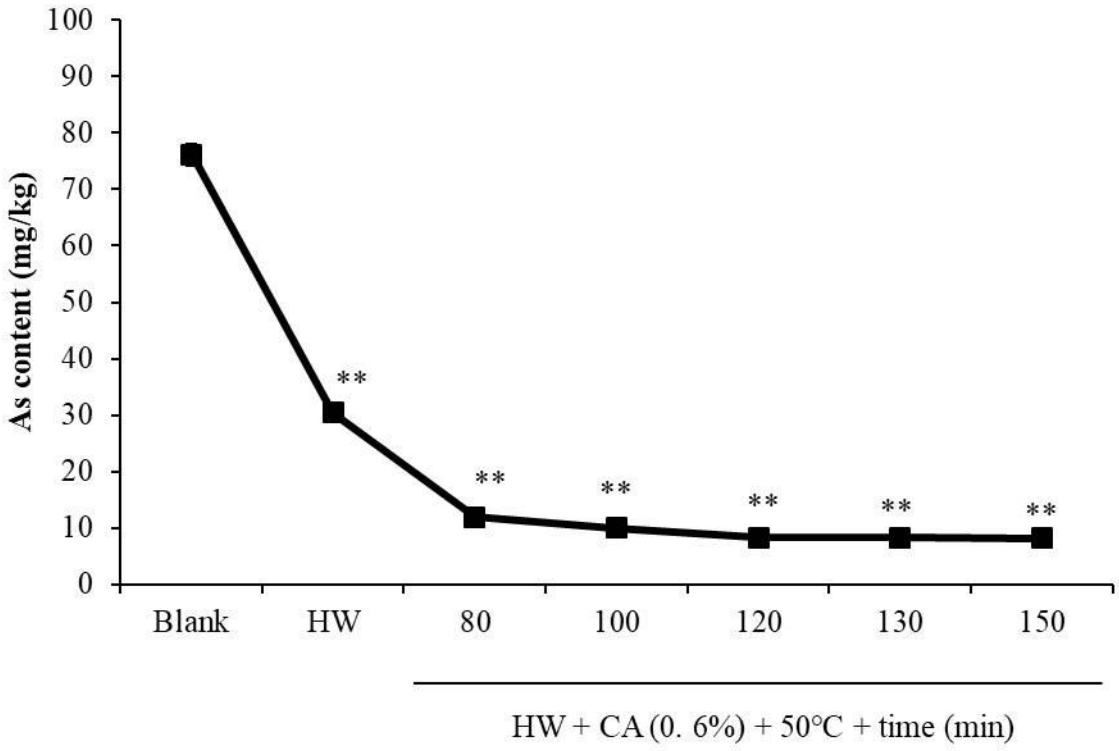

Fig. 3. As content of *H. fusiforme* after CA-processing by different times. ***p*<0.01 compared to blank group.

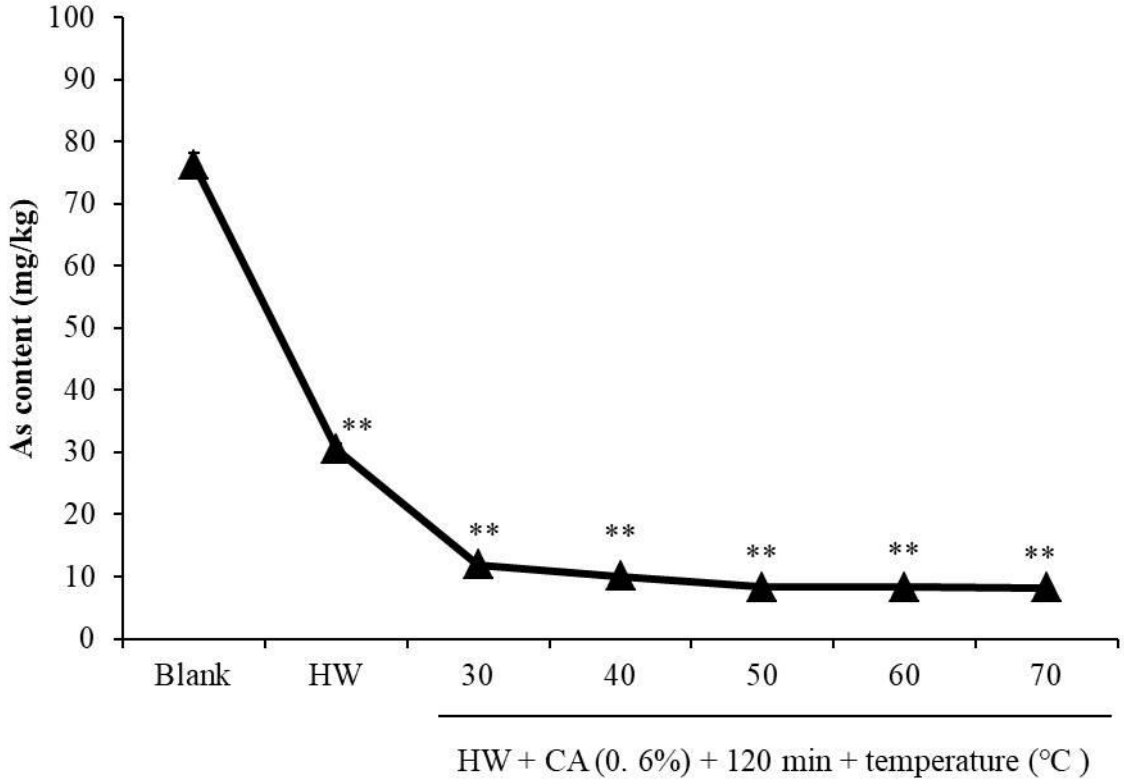

Fig. 4. As content of *H. fusiforme* after CA-processing by different temperatures. ***p*<0.01 compared to blank group.

2.3. Processing optimization using RSM

Based on the results of the single-factor experiments, CA concentration (0.2-1.0%), processing time (80-150 min), and processing temperature (30-70 ℃) were selected for the optimization of the As content of *H. fusiforme*. A group of 17 experiments was executed in analogy with the Box-Behnken design. The variables of actual and coded levels as well as of As content are shown in Table 3. A quadratic equation was used to establish a statistical model to confirm the optimum conditions and the response of the combined factors. By using multiple regression analysis on the experimental data, the yield of polyphenol was obtained using the following quadratic equation:

$$R=2.26-0.086A-0.45B-0.074C+0.31AB-0.059AC+0.13BC+0.36A^2+0.62B^2+0.37C^2$$

Y was the predicted response; A was the CA concentration; B was the processing time; C was the processing temperature.

Variance analysis was conducted for the above regression model, and significance test was conducted for the model coefficients, as shown in table 4. *F* value was used to test the significance of the influence of each variable on the response value. The smaller *P* was the higher the significance of the corresponding variable, while the unfitting term *P* > was not significant at 0.05. According to the results of ANOVA in Table 4, F =68.03, $p < 0.0001$ had a significant difference, and the unfitting term p=0.1354>0.05, and R^2=0.9887, indicating that the model had a good fitting degree. Meanwhile, the adjoint determination coefficient (R^2_{Adj}=0.9742), determination coefficient (R^2=0.8654) of the method was reliable and could be used to analyze and predict the optimal processing of As content.

Base on Table 4, the concentration of CA and processing time had significant influence on the content of As (P<0.05), but the effect of temperature on the content of As was not significant (P>0.05). In addition, the influence degree of factors on the content of As was

B>A>C. For the interaction, the effect of the concentration of CA and processing time, and the interaction of time and temperature on the content of As was significant (P <0.05), but the effect of the interaction of concentration of CA and processing temperature on the content of As was not significant (P>0.05). For the quadratic terms, the results are extremely significant. In addition, according to the response surface figures (Fig. 5) are opening up paraboloid, thus, there is minimum. In order to further optimize the results, a conclusion according to the Design-Expert software in concentration of CA, processing time and temperature under the influence of the interaction. The results indicated that the optimum processing condition as: the CA concentration is 0.39%; the processing time is 129.26 min; the processing temperature is 58.68 ℃, under the condition of the model to predict the content of As is 2.193 mg/kg.

Table 3. Response and experiment design of As content of after CA processing

Run	Experimental factor			As content (mg/kg)
	A	B	C	
1	0.000	1.000	1.000	2.822
2	1.000	0.000	-1.000	2.973
3	-1.000	0.000	-1.000	3.159
4	0.000	0.000	0.000	2.328
5	0.000	-1.000	-1.000	3.950
6	-1.000	0.000	1.000	3.140
7	0.000	0.000	0.000	2.230
8	1.000	-1.000	0.000	3.335
9	1.000	1.000	0.000	3.120
10	-1.000	1.000	0.000	2.539
11	0.000	0.000	0.000	2.215
12	0.000	1.000	-1.000	2.730
13	1.000	0.000	1.000	2.719
14	0.000	0.000	0.000	2.201
15	0.000	0.000	0.000	2.338
16	-1.000	-1.000	0.000	3.999
17	0.000	-1.000	1.000	3.540

Table 4. ANOVA of the quadratic polynomial model and significant test.

Source	Sum of		Mean	*F*	*P*-value	Significance
	Squares	df	Square	Value	*p*	
Model	5.27	9	0.59	68.03	< 0.0001	**
A	0.060	1	0.060	6.91	0.0340	*
B	1.63	1	1.63	189.40	< 0.0001	**
C	0.044	1	0.044	5.07	0.0591	
AB	0.39	1	0.39	44.98	0.0003	*
AC	0.014	1	0.014	1.60	0.2460	
BC	0.063	1	0.063	7.31	0.0305	*
$\mathbf{A^2}$	0.55	1	0.55	63.89	< 0.0001	**
$\mathbf{B^2}$	1.64	1	1.64	190.48	< 0.0001	**
$\mathbf{C^2}$	0.59	1	0.59	68.29	< 0.0001	**
Residual	0.060	7	0.009			
Luck of fit	0.043	3	0.014	3.37	0.1354	
Pure error	0.017	4	0.004			
Cor total	5.34	16				

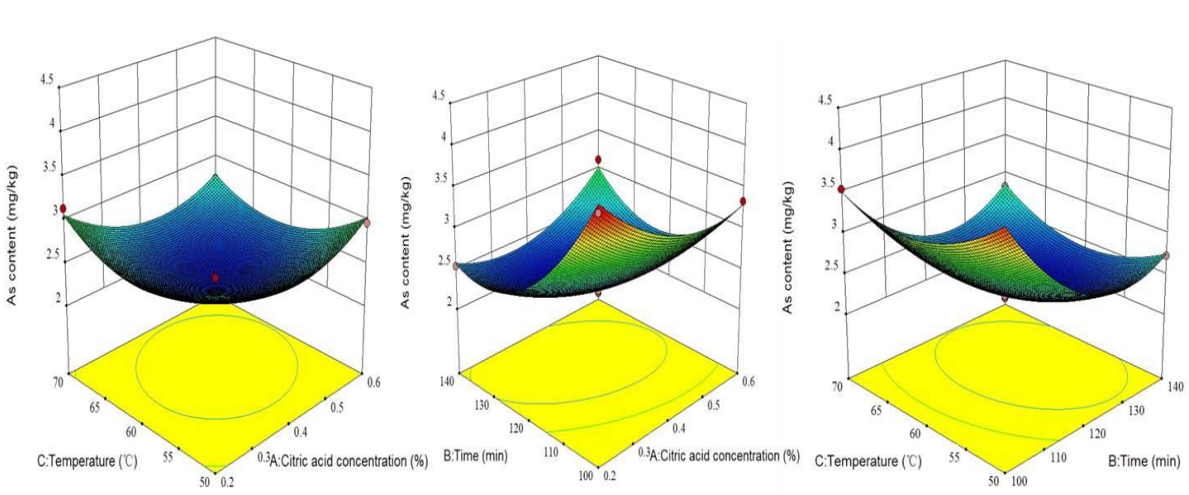

Fig. 5. Response surface plots of variable parameters on the As content of *H. fusiforme*.

3. Summary

The As content of *H. fusiforme* could be successful removed by CA-processing. Optimal processing condition has been investigated by response surface methodology experiment. The results indicated that the optimum processing condition as: the CA concentration is 0.39%; the processing time is 129.26 min; the processing temperature is 58.68 ℃, under the condition of the model to predict the content of As is 2.193 mg/kg. In addition, according to the actual experiment and industrial production condition, the processing conditions are finally determined as: the CA concentration is 0.4%; the processing time is 120 min; the processing temperature is 60 ℃.

Part II.

Fermentation of acid-processed *H. fusiforme*

Part II.

Fermentation of acid-processed *H. fusiforme*

Abstract

The previous study suggested that As of *H. fusiforme* could be removed by CA-processing. To further remove of the As from *H. fusiforme*, the CA-processed *H. fusiforme* was fermented by different of probiotics. The As contents and the reducing capacities of fermented have been investigated. The results indicated that the *H. fusiforme* fermented by *Lactobacillus rhamnosus* possesses the lowest As content and highest reducing capacity. Therefore, *Lactobacillus rhamnosus* was selected as the strain to fermentation of CA-processed *H. fusiforme*. In addition, the chemical composition and bioactivities of non-fermented and fermented *H. fusiforme* were investigated. The results displayed that the bioactivities of *H. fusiforme* were increased after fermentation and the main composition of fermented *H. fusiforme* is polysaccharides.

1. Materials and methods

1.1. Reagents and chemicals

CA-processed *H. fusiforme* was prepared by previous study. *Lactobacillus plantarum* (ATCC® 8014™), *Lactobacillus rhamnosus* (ATCC® 21052™), and yeast (ATCC® 24060™) were purchased from ATCC (American Type Culture Collection, Manassas, VA, USA). MRS broth medium and tryptone were purchased from Sigma Co. (St. Louis, MO, USA). All other chemicals and reagents were analytical grade.

1.2. Activation of probiotics

MRS broth medium was weighed according to the formula quantity, dissolved in water, and was separated into 40 mL/ bottle. The medium were sterilized at 121℃ for 20 min. The preserved strain glycerin tube was inoculated into MRS broth medium at 1% (V/V) and activated in a biochemical incubator at 37℃ for 18h.

1.3. Fermentation of CA-processed *H. fusiforme*

The protocol for fermentation of CA-processed *H. fusiforme* was shown as Fig. 6. In brief, the CA-processed was homogenised with 4-folds of water (W/V) and adjusted the pH to 6.5 by KOH (1 M) solution, and then sterilized. The sterilized *H. fusiforme* solution was inoculated with 5% of different strains (Table 5) and incubated in a biochemical incubator at 37℃ for 48h. After fermentation, the solutions were centrifuged (5000 rpm, 6 min) and filtrated. Finally, the supernatant was collected and dried; the fermented *H. fusiforme* samples were obtained.

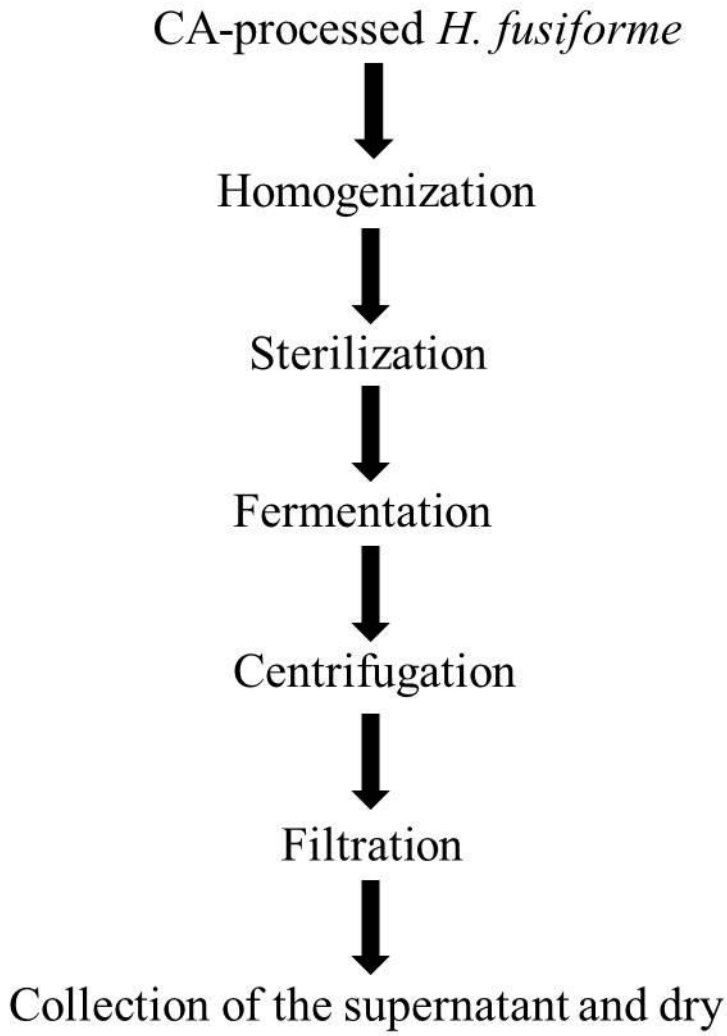

Fig. 6. The protocol of fermentation.

1.4. Measurement of the reducing capacities of fermented *H. fusiforme* samples

The reducing capacities of fermented *H. fusiforme* samples were measured by Prussian-blue Iron Stain assay [65, 66]. Precision absorb respectively before and after fermentation supernatant 1 mL (5000 RPM, centrifugal 6 min), add 2.5 mL of phosphate buffer (0.2 mol/L, pH 6.6) and 2.5 mL of potassium ferricyanide solution (1%). The mixture was heated at 50℃ in the water bath and cooled after 20 min. Add 2.5 mL of trichloroacetic acid solution (10%), and then transfer 2.5 mL of the mixture in colorimetric tube. Distilled water (2.5 mL) and ferric chloride solution (0.1%, 0.5 mL) were added into colorimetric tube, and keep 10 min in the room temperature for reaction. Finally, the absorbance of the reaction mixture at 700 nm was measured.

1.5. Fermentation of CA-processed *H. fusiforme* by *Lactobacillus rhamnosus* in different times

The CA-processed *H. fusiforme* was fermented by *Lactobacillus rhamnosus* for 24, 36, 48, 60 and 72 h following the protocol described in 1.3. In addition, the reducing capacities of *Lactobacillus rhamnosus*-fermented *H. fusiforme* by different times were measured by Prussian-blue Iron Stain assay followed the methods described in 1.4.

1.6. Preparation of non-fermented and fermented samples

After confirm the fermentation condition, the non-fermented (HF) and fermented (HFF) *H. fusiforme* extracts were prepared for further study following the protocols described in Fig. 7.

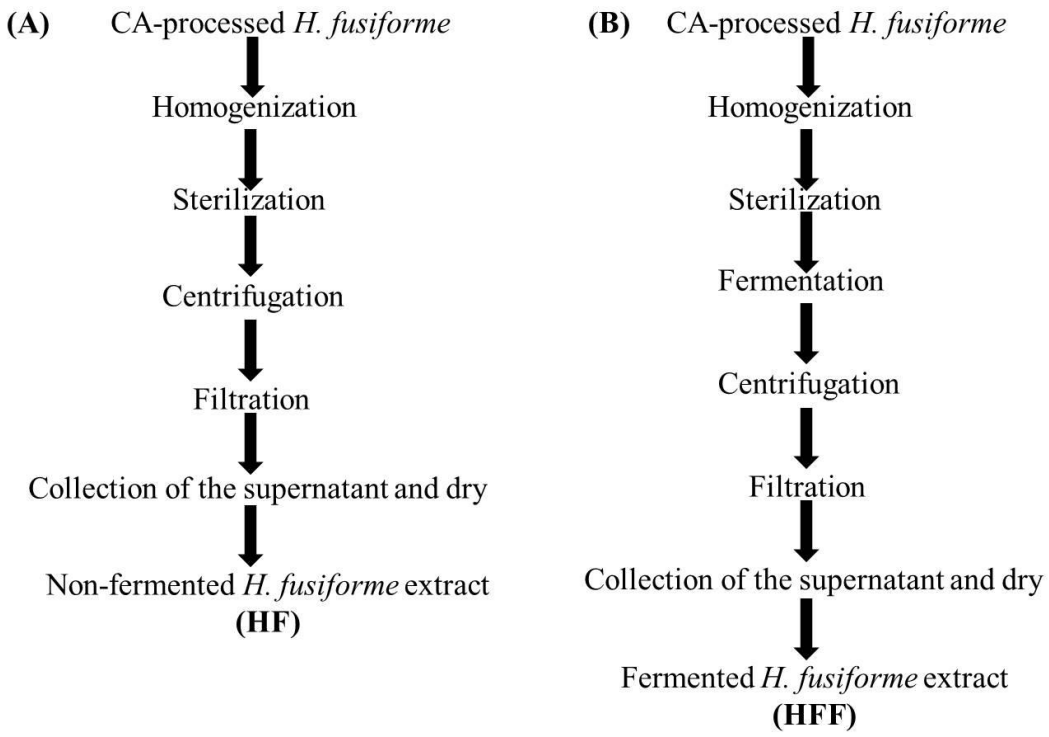

Fig. 7. Preparation of (A) non-fermented and (B) fermented *H. fusiforme* extract.

1.7. Chemical analysis

The total carbohydrate, phenolic, and protein content of samples were determined based on the protocol of official methods for analysis of the Association of Official Analytical Chemists (AOAC) [67].

1.8. Measurement of As content of fermented acid-processed *H. fusiforme*

The As content was determined by Hydride Generation-Atomic Fluorescence Spectrometer (HG-AFS) [31, 61-63]. Samples of 0.1g (up to 0.001g) were weighed into a 25 mL colorimetric tube and mixed with 50% hydrochloric acid solution and sonication. The sample was fully extracted after 20 min, and then taken out for cooling and filtration. Taken 2 mL of sample solution and placed in 10 mL colorimetric tube, 1 mL of thiourea (5%) and ascorbic acid (5%) solution was added. The volume was fixed with deionized water and the solution was shaken and placed for 20 min to be tested. After preheating for 20~30min, the atomic fluorescence spectrometer started the measurement, followed by standard series measurement and sample measurement, and the reagent space ratio experiment.

1.9. Measurement of DPPH radical scavenging activity

The DPPH radical scavenging activities of samples were determined by colorimetric methods. The reaction mixture containing 100 μL of DPPH solution (0.4 mM) and 100 μL sample solutions was incubate at room temperature for 30 min. After incubation, the absorbance was recorded at 517 nm using an ELISA microplate reader (Olympus, Japan).

1.10. Measurement of hydrogen peroxide scavenging activity

The hydrogen peroxide scavenging activities of samples were determined by colorimetric methods. The reaction mixture containing 50 μL of 0.1 M phosphate buffer (pH 5), 50 μL sample solutions was mixed with different concentrations and 10 μL of 10 mM hydrogen peroxide. After filled above solution in 96-well plate, the plate was incubated at 37 ℃ for 5 min. After incubation, 15 μL of 1.25 mM ABTS and 15 μL of peroxidase were added into the plate, and incubate at 37 ℃ for 10 min. After incubation, the absorbance was recorded at 405 nm using an ELISA microplate reader (Olympus, Japan).

1.11. Determination of the cytotoxicity on Vero cells

To evaluate the cytotoxicity of HF and HFF, Vero cells were seeded and incubated for 24 h. Cells were treated with 10 μL of samples to final concentrations of 25, 50, and 100 μg/mL, and incubated for 24 h at 37 ℃. Cell viability was estimated using an MTT assay as described by Fernando et al. [18].

1.12. Determination of the protective effect of HF and HFF against H_2O_2-induced intracellular ROS generation in Vero cells

Vero cells were seeded as described above, and cultured for 24 h. Different concentrations of HF and HFF were added to cells prior to incubation for 1 h. After incubation, H_2O_2 (1 mM) was added to the cells, followed by incubation for 1 h. Finally, DCFH-DA (500 μg/mL) was introduced to the cells, and the fluorescence emission of DCF-DA was detected using a fluorescence a microplate reader (Olympus, Japan).

1.13. Measurement of the protective effect of HF and HFF against H_2O_2-induced cytotoxicity in Vero cells

Vero cells were seeded in a 96-well plate as described above. After 24 h incubation, cells were treated with different concentrations of HF and HFF and incubated for 1 h. After incubation, H_2O_2 (1 mM) was added to the cells prior to incubation for 24 h. Cell viability was measured by MTT assay, according to Fernando et al. [18].

1.14. Measurement of NO production and cell viability in LPS-stimulated RAW 264.7 cells

The experiments were performed following the methods described by Heo et al. [9]. RAW 264.7 cells were seeded in a 24-well plate for 24 h. HF and HFF was added into each well, achieving final concentrations of 25, 50, and 100 μg/mL. After 1 h, LPS (1 μg/mL) was introduced into all wells, except control. After 24 h, 100 μL of the culture medium from each well was transferred to a 96-well plate and mixed with 100 μL Griess reagent (1% sulfanilamide and 0.1% naphthylethylenediamine dihydrochloride in 2.5% phosphoric acid). The absorbance was read on a microplate reader after 10 minutes, at a wavelength of 540 nm. In addition, 100 μL of MTT solution (2 mg/mL) was added to the remaining cells in the 24-well plate, and incubated for 3 h. The resulting formazan crystals of MTT were then dissolved in DMSO and absorbance was determined using a microplate reader at a wavelength of 540 nm [68].

1.15. Statistical analysis

All the experiments were performed in triplicate. The data were expressed as the mean ± standard error (SE), and one-way ANOVA test (using SPSS 12.0 statistical software) was used to statistically compare the mean values of each treatment. Significant differences

between the means of parameters were determined by Duncan's multiple range tests, $p < 0.05$ and $p < 0.01$ were considered as significantly different.

2. Results and discussion

2.1. The reducing capacities of fermented *H. fusiforme*

The reducing capacities of *H. fusiforme* fermented by different stains were measured and the results were summarized in Table 5. As the results shown, *Lactobacillus rhamnosus* fermented *H. fusiforme* were shown strongest activity in all of samples. Thus, *Lactobacillus rhamnosus* was selected as the target stain to fermentation of *H. fusiforme*.

To investigate the optimal fermentation time, *H. fusiforme* was fermented with *Lactobacillus rhamnosus* for different times, and the reducing capacities of different fermented *H. fusiforme* samples were measured. As Table 6 shows, *H. fusiforme* fermented by *Lactobacillus rhamnosus* for 48 h sample possesses strongest reducing capacity than other samples. Base on this result, the optimal fermentation time of *H. fusiforme* was determined as 48 h.

2.2. Chemical and element composition of processed *H. fusiforme*

The chemical and element composition of normal, CA-processed, and fermented *H. fusiforme* were compared in this study, the results were summarized in Table 7. As the results shown, non-fermented sample contain a high amount of As, however, the As content was effected reduced by CA-processing and fermented. This result indicated that As of *H. fusiforme* could be effectively removed by CA-processing and fermented. In addition, Fe content of *H. fusiforme* was also been removed during processing. Furthermore, the chemical composition analysis of *H. fusiforme* samples displayed that all of those *H. fusiforme* samples were rich in polysaccharides.

Table 5. The fermentation condition *H. fusiforme* fermented by different bacteria.

Number	Strain	Inoculation amount	Fermentation time	Reducing capacity
1	Non-fermented	0%	48h	0.887
2	*Lactobacillus plantarum* (ATCC® 8014™)	5%	48h	1.200
3	*Lactobacillus rhamnosus* (ATCC® 21052™)	5%	48h	1.494
4	Yeast (ATCC® 24060™)	5%	48h	0.857
5	*Lactobacillus plantarum* *Lactobacillus rhamnosus*	5%	48h	1.295
6	*Lactobacillus plantarum* Yeast	5%	48h	0.903
7	*Lactobacillus rhamnosus* Yeast	5%	48h	1.053
8	*Lactobacillus plantarum* *Lactobacillus rhamnosus* Yeast	5%	48h	1.105

Table 6. The fermentation condition *H. fusiforme* fermented by *Lactobacillus rhamnosus*.

No.	**Strain**	**Inoculation amount**	**Fermentation time**	**Reducing capacity**
1	*Lactobacillus rhamnosus*	5%	24h	1.149
2	*Lactobacillus rhamnosus*	5%	36h	1.403
3	*Lactobacillus rhamnosus*	5%	48h	1.504
4	*Lactobacillus rhamnosus*	5%	60h	1.287
5	*Lactobacillus rhamnosus*	5%	72h	1.114

Table 7. Chemical and element composition of processed *H. fusiforme*.

Content	Unit	Non-processed	CA-processed	CA-processed & Fermentation
Protein	%	11.22	12.43	13.09
Moisture	%	6.77	6.99	6.6
Carbohydrate	%	31.56	46.14	52.05
As	mg/kg	76.18	2.204	1.64
Fe	mg/kg	286	336	189
Cu	mg/kg	5.97	10.4	9.26
Ca	mg/kg	16300	11700	16200
Zn	mg/kg	16.4	24.7	15.9
Na	mg/100g	3280	890	418
Mn	mg/kg	12.8	15.0	10.6
Mg	mg/kg	7540	5340	3860
K	mg/kg	118000	34300	13000

2.3. Chemical composition of HF and HFF

HF and HFF were prepared (Fig. 7). As shown in Table 8, HF contains 1.18±0.14% of phenolic content and 46.14±0.76% of polysaccharides content; and HFF contains 2.84±0.14% of phenolic content and 52.05±1.52% of polysaccharides content. These results indicated that both phenolic and polysaccharide content were increased after fermentation.

2.4. Antioxidant activities of HF and HFF

Antioxidant activities of HF and HFF have evaluated by investigating the DPPH radical and hydrogen peroxide scavenging activities, as well as the effects of HF and HFF in H_2O_2-induced Vero cells. As the results shown, HF and HFF shows strong DPPH radical scavenging activity, as well as hydrogen peroxide scavenging activity (Fig. 8 A and B). HFF has shown stronger DPPH radical and hydrogen peroxide scavenging activities then HF.

The cytotoxicity of HF and HFF on Vero cells were determined. As shown in Fig. 9, HF and HFF were not shown toxicity on Vero cells. In addition, HFF was shown significantly proliferation effect at the high concentration (200 μg/mL). Thus, the highest concentrations of HF and HFF for further studies were performed as 100 μg/mL.

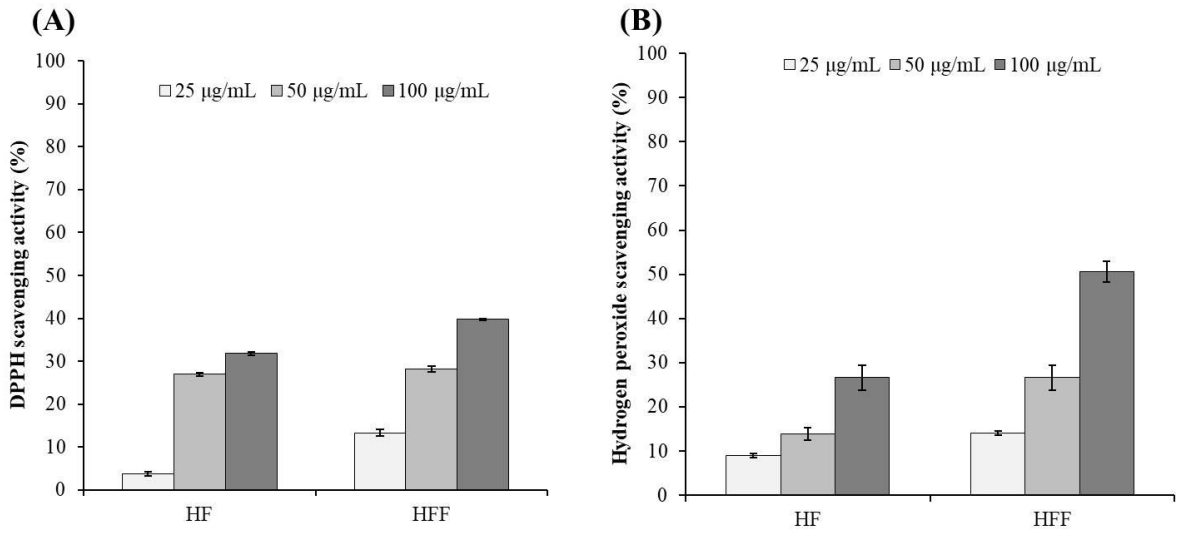

Fig. 8. (A) DPPH radical and (B) hydrogen peroxide scavenging activities of HF and HFF.

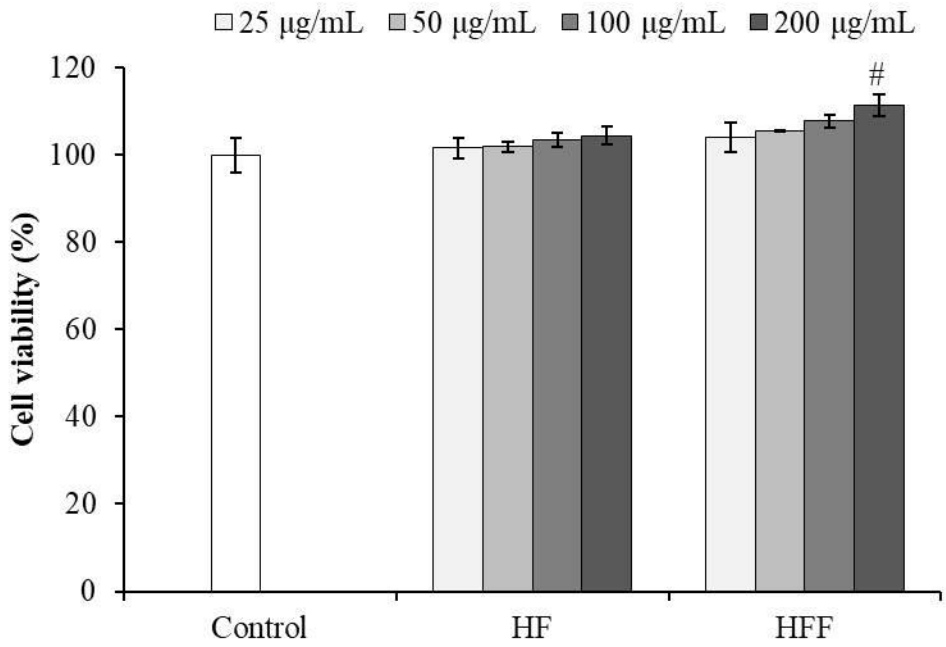

Fig. 9. Cytotoxicity of HF and HFF on Vero cells. Cell viability was measured by MTT assay. The experiments were conducted in triplicate, and the data are expressed as the mean ± standard error (SE). # $p < 0.05$ as compared to the control group.

2.5. Protective effects of HF and HFF against H_2O_2-induced oxidative stress in Vero cells

As shown in Fig. 10, the intracellular ROS level significantly increased (Fig. 10A), and cell viability decreased (Fig. 10B) following treatment with H_2O_2. However, the intracellular ROS levels were decreased, and cell viabilities were increased, following treatment at all measured concentrations of HF and HFF. Both effects occurred in a dose-dependent manner. These result indicated that HF and HFF possess strong antioxidant activity in H_2O_2-induced Vero cells. In addition, HFF possesses stronger antioxidant activity than HF.

2.6. The effect of HF and HFF on LPS-induced NO generation and cytotoxicity in RAW 264.7 macrophages

LPS is a component of the cell wall in gram-negative bacteria, which stimulates inflammatory responses in macrophages. Therefore, LPS-stimulated RAW 264.7 cells are an excellent choice for investigating the anti-inflammatory activities of HF and HFF. The effects of HF and HFF on NO generation and cytotoxicity were measured in LPS-induced RAW 264.7 macrophages. As shown in Fig. 11, HF and HFF significant inhibits NO generation in LPS-induced RAW 264.7 cells (Fig. 11A). In addition, HF and HFF remarket improves cell viability (Fig. 11B). Both effects were dose-dependent. These results displayed that HF and HFF possess strong anti-inflammatory effects in LPS-induced RAW 264.7 cells. Furthermore, HFF possesses stronger anti-inflammatory effects than HF.

The above results indicated that HFF possesses stronger antioxidant and anti-inflammatory effects than HF. It suggested that the bioactivity of *H. fusiforme* was increased after fermentation.

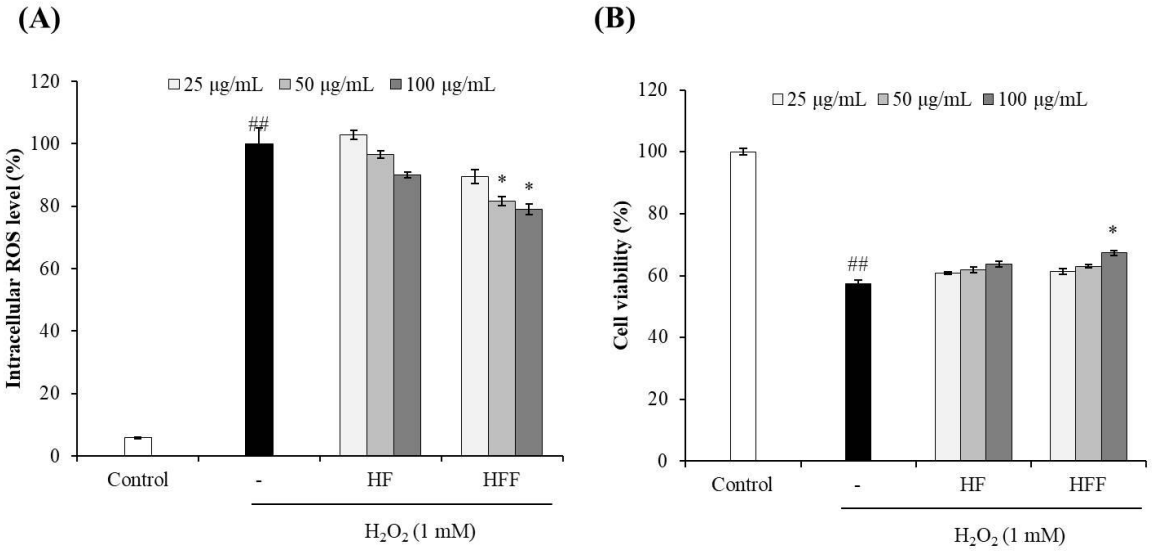

Fig. 10. The intracellular ROS scavenging effect of HF and HFF during H_2O_2-induced oxidative stress in Vero cells (A) and the protective effects of HF and HFF against H_2O_2-induced cell death in Vero cells (B). The experiments were conducted in triplicate, and the data are expressed as the mean ± SE. $^{*}p < 0.05$ as compared to the H_2O_2-treated group and $^{\#\#}p < 0.01$ as compared to the control group.

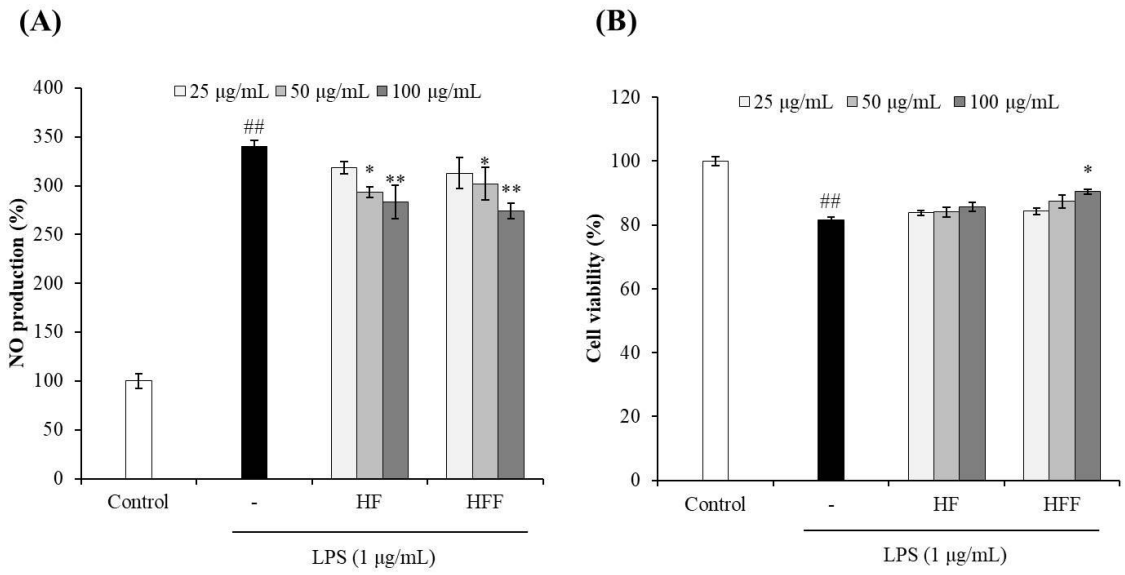

Fig. 11. The effect of HF and HFF on LPS-induced NO generation and cytotoxicity in RAW 264.7 macrophages. (A) NO production in LPS-induced RAW 264.7 macrophages and (B) Cell viability in LPS-induced RAW 264.7 macrophages. The experiments were conducted in triplicate, and the data are expressed as the mean ± SE. *$p < 0.05$, ** $p < 0.01$ as compared to the LPS-treated group and $^{\#\#}p < 0.01$ as compared to the control group.

3. Summary

The optimal fermentation condition of *H. fusiforme* was confirmed. The As contents and the reducing capacities of fermented have been investigated. The results indicated that the *H. fusiforme* fermented by *Lactobacillus rhamnosus* possesses the lowest As content and highest reducing capacity. Therefore, *Lactobacillus rhamnosus* was selected as the strain to fermentation of CA-processed *H. fusiforme*. In addition, the chemical composition and bioactivities of non-fermented and fermented *H. fusiforme* were investigated. The results displayed that the bioactivities of *H. fusiforme* were increased after fermentation and the main composition of fermented *H. fusiforme* is polysaccharides. However, the polysaccharides of fermented *H. fusiforme* have to be further purified and the activities of the purified polysaccharide need to be investigated.

Part III.

Isolation, purification, and characterization of polysaccharides from fermented *H. fusiforme*

Part III.

Isolation, purification, and characterization of polysaccharides from fermented *H. fusiforme*

Abstract

The crude polysaccharides (HFF-PS) of fermented *H. fusiforme* (HFF) were separated by ethanol precipitation. HFF-PS contains high amount polysaccharides (60.63%) and sulfated content (17.18%), as well as possesses strong antioxidant and anti-inflammatory activity. Thus, it has been further purified. After purification, an active fraction (HFF-PS-F5) was separated from the crude polysaccharides (HFF-PS) from fermented *H. fusiforme*. HFF-PS-F5 contains 91.68% sulfated polysaccharides, which comprise fucose (53.84%), galactose (19.08%), glucose (2.22%), and mannose (24.86%). In addition, the characteristics of HFF-PS-F5 had been determined by Fourier-transform infrared (FT-IR) and HPGPC. The results indicated that HFF-PS-F5 is the fucoidan with an average molecular weight as 213.33 kDa. The bioactivities of HFF-PS-F5 need be further investigated.

1. Materials and methods

1.1. Reagents and chemicals

Trifluoroacetic acid, arabinose, fucose, galactose, glucose, rhamonose, and xylose were purchased from Sigma (Sigma, St. Louis, MO, USA). 1-diphenyl-2-picrylhydrazyl (DPPH), gallic acid, LPS, and glucose were purchased from Sigma Co. (St. Louis, MO, USA). The 3-(4-5-dimethyl-2yl)-2-5-diphynyltetrasolium bromide (MTT), fluorescent probe 2', 7'-dichlorodihydroflurescin diacetate (DCFH-DA), dimethyl sulfoxide (DMSO), and acridine orange were purchased from Sigma (St. Louis, MO, USA). H_2O_2 was purchased from Fluka Co. (Buchs, Switzerland). Vero cells were purchased from the Korea Cell Line Bank (KCLB, Seoul, Korea) and RAW 264.7 macrophages were purchased from ATCC (TIB-71^{TM}). Dulbecco's modified Eagle's medium (DMEM), RPMI-1640 medium, FBS, penicillin-streptomycin, and trypsin-EDTA were purchased from Gibco-BRL (Grand Island, NY, USA). All other chemicals and reagents were analytical grade.

1.2. Separation of crude polysaccharides from HFF

As Fig. 12 shows, the CA-processed *H. fusiforme* was fermented. After fermentation, HFF was obtained. HFF was precipitated by ethanol, and then the crude polysaccharides of HFF were obtained and referred as HFF-PS.

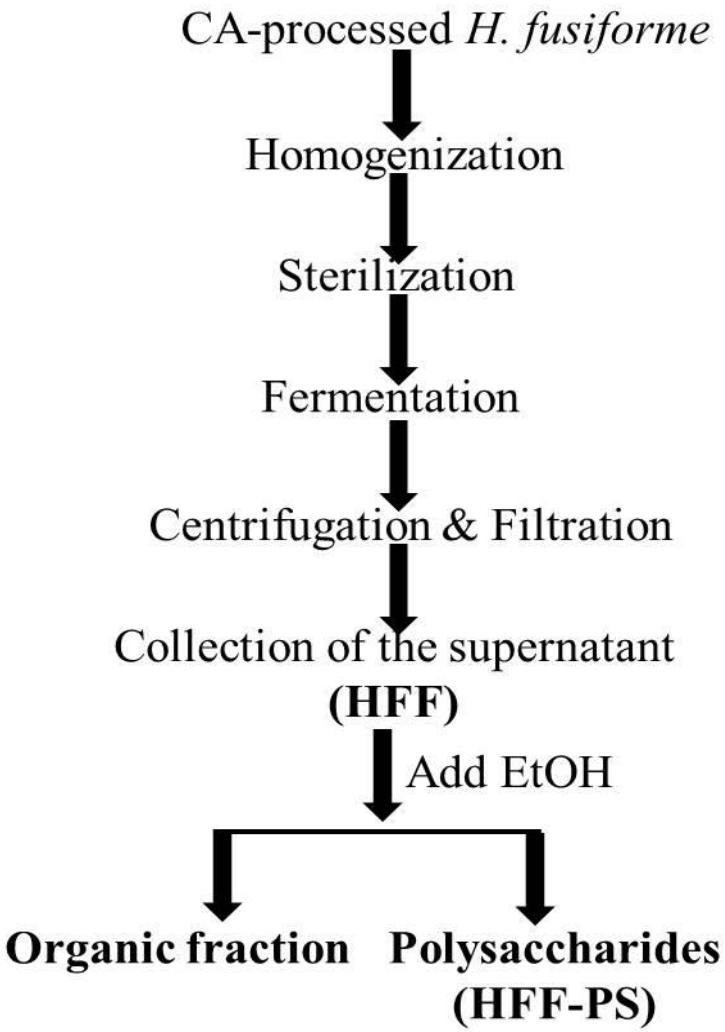

Fig. 12. Separation of polysaccharides from fermented *H. fusiforme* extract.

1.3. Isolation fucoidan from HFF-PS

HFF-PS was loaded to a DEAE-cellulose column and eluted by NaCl containing sodium acetate (50 mM, pH 5.0). The elution was carried out with a gradient of NaCl (0~2 M, 30 mL/h). Each 10 mL eluent was collected, and the polysaccharide content of each fraction was measured using phenol–H_2SO_4 assay. The polysaccharide fractions were pooled, dialyzed and freeze-dried.

1.4. Chemical analysis

The total carbohydrate and phenolic content of samples were determined based on the protocol of official methods for analysis of the Association of Official Analytical Chemists (AOAC) [67]. To determine the sulfate content, samples were hydrolyzed by 4 M trifluoroacetic acid at 100 ℃ for 5 hours. The sulfate content was measured by the method described by Wang et al. [47]. In order to analyze the monosaccharide components of target sample, the sample was hydrolyzed by 4 M of trifluoroacetic acid in sealed glass vials for 4 h at 100 ℃. Then, the neutral sugar component of HFPS-F4 was determined by HPAE-PAD base on the procedure described in the previous studies **[68, 69]**.

1.5. Fourier-transform infrared (FT-IR) analysis

The IR spectrum of target sample and commercial fucoidan were recorded using a FT-IR spectrometer (Nicolet™ 6700 FT-IR spectrometer; Madison, WI, USA). Samples were separately homogenized with KBr, and then the mixture were pressed into pellets for FT-IR measurement in the frequency range of 500~2000 cm^{-1}.

1.6. Molecular weight analysis

The molecular weight (Mw) of target sample was analysis by HPGPC (high-performance gel permeation chromatography) with two types of size-exclusion chromatography columns in series, namely TSKgel 2500PW_{xl} (7.8×300 mm, Tosoh Co., Ltd., Tokyo, Japan) and TSKgel $GMPW_{xl}$ (7.8×300 mm, Tosoh Co., Ltd., Tokyo, Japan), on a Waters HPLC system (Waters, USA) equipped with a Waters 2414 differential refractive index detector [70]. The sample solution (3 mg/mL, 200 μL) filtered through a Nylon filter (0.45 μm). Filtered sample solution (20 μL) were injected with column and eluted with $NaNO_3$ (0.1 M, 1 mL/min; 60 min, 40 ℃). The Mw of sample was calculated by the calibration curve obtained using various standard dextran.

1.7. Measurement of DPPH radical scavenging activity

The DPPH radical scavenging activities of samples were determined by colorimetric methods. The reaction mixture containing 100 μL of DPPH solution (0.4 mM) and 100 μL sample solutions was incubate at room temperature for 30 min. After incubation, the absorbance was recorded at 517 nm using an ELISA microplate reader (Olympus, Japan).

1.8. Measurement of hydrogen peroxide scavenging activity

The hydrogen peroxide scavenging activities of samples were determined by colorimetric methods. The reaction mixture containing 50 μL of 0.1 M phosphate buffer (pH 5), 50 μL sample solutions was mixed with different concentrations and 10 μL of 10 mM hydrogen peroxide. After filled above solution in 96-well plate, the plate was incubated at 37 ℃ for 5 min. After incubation, 15 μL of 1.25 mM ABTS and 15 μL of peroxidase were added

into the plate, and incubate at 37 ℃ for 10 min. After incubation, the absorbance was recorded at 405 nm using an ELISA microplate reader (Olympus, Japan).

1.9. Determination of the cytotoxicity on Vero cells

To evaluate the cytotoxicity of HFF-PS, Vero cells were seeded and incubated for 24 h. Cells were treated with 10 μL of samples to final concentrations of 25, 50, and 100 μg/mL, and incubated for 24 h at 37 ℃. Cell viability was estimated using an MTT assay as described by Fernando et al. [18].

1.10. Determination of the protective effect of HFF-PS against H_2O_2-induced intracellular ROS generation in Vero cells

Vero cells were seeded as described above, and cultured for 24 h. Different concentrations of HFF-PS were added to cells prior to incubation for 1 h. After incubation, H_2O_2 (1 mM) was added to the cells, followed by incubation for 1 h. Finally, DCFH-DA (500 μg/mL) was introduced to the cells, and the fluorescence emission of DCF-DA was detected using a fluorescence a microplate reader (Olympus, Japan).

1.11. Measurement of the protective effect of HFF-PS against H_2O_2-induced cytotoxicity in Vero cells

Vero cells were seeded in a 96-well plate as described above. After 24 h incubation, cells were treated with different concentrations of HFF-PS and incubated for 1 h. After incubation, H_2O_2 (1 mM) was added to the cells prior to incubation for 24 h. Cell viability was measured by MTT assay, according to Fernando et al. [18].

1.12. Measurement of NO production and cell viability in LPS-stimulated RAW 264.7 cells

The experiments were performed following the methods described by Heo et al. [9]. RAW 264.7 cells were seeded in a 24-well plate for 24 h. HFF-PS was added into each well, achieving final concentrations of 25, 50, and 100 μg/mL. After 1 h, LPS (1 μg/mL) was introduced into all wells, except control. After 24 h, 100 μL of the culture medium from each well was transferred to a 96-well plate and mixed with 100 μL Griess reagent (1% sulfanilamide and 0.1% naphthylethylenediamine dihydrochloride in 2.5% phosphoric acid). The absorbance was read on a microplate reader after 10 minutes, at a wavelength of 540 nm. In addition, 100 μL of MTT solution (2 mg/mL) was added to the remaining cells in the 24-well plate, and incubated for 3 h. The resulting formazan crystals of MTT were then dissolved in DMSO and absorbance was determined using a microplate reader at a wavelength of 540 nm [68].

1.13. Statistical analysis

All the experiments were performed in triplicate. The data were expressed as the mean ± standard error (SE), and one-way ANOVA test (using SPSS 12.0 statistical software) was used to statistically compare the mean values of each treatment. Significant differences between the means of parameters were determined by Duncan's multiple range tests, $p < 0.05$ and $p < 0.01$ were considered as significantly different.

2. Results and discussion

2.1. Chemical composition of HFF-PS

HFF-PS was successful isolated by ethanol precipitation (Fig. 12). As shown in Table 9, HFF-PS contains 0.00±0.15% of phenolic content, 60.63±3.04% of polysaccharides, and 17.18±0.31% of sulfate content, respectively. Altogether, HFF-PS contains 77.81% sulfated polysaccharides.

2.2. Antioxidant activity of HFF-PS

Antioxidant activity of HFF-PS has evaluated by investigating the DPPH radical and hydrogen peroxide scavenging activities, as well as the effect of HFF-PS in H_2O_2-induced Vero cells. As the results shown, HFF-PS shows strong DPPH radical scavenging activity, as well as hydrogen peroxide scavenging activity (Fig. 13 A and B). The cytotoxicity of HFF-PS on Vero cells was determined. As shown in Fig. 14, HFF-PS has not shown toxicity on Vero cells, as well as shown proliferation effect at the high concentration (200 μg/mL). Thus, the highest concentration of HFF-PS for further studies has been performed as 100 μg/mL.

2.3. Protective effect of HFF-PS against H_2O_2-induced oxidative stress in Vero cells

As Fig. 15 shows, the intracellular ROS level significantly increased (Fig. 15A), and cell viability decreased (Fig. 15B) following treatment with H_2O_2. However, the intracellular ROS levels were decreased, and cell viabilities were increased, following treatment at all measured concentrations of HFF-PS. Both effects occurred in a dose-dependent manner. These result indicated that HFF-PS possesses strong antioxidant activity in H_2O_2-induced Vero cells.

Table 9. Chemical composition of HFF-PS obtained from HFF.

Composition (%)	HFF-PS
Phenolic content	0.00±0.15
Carbohydrate content	60.63±3.04
Sulfate content	17.18±0.31

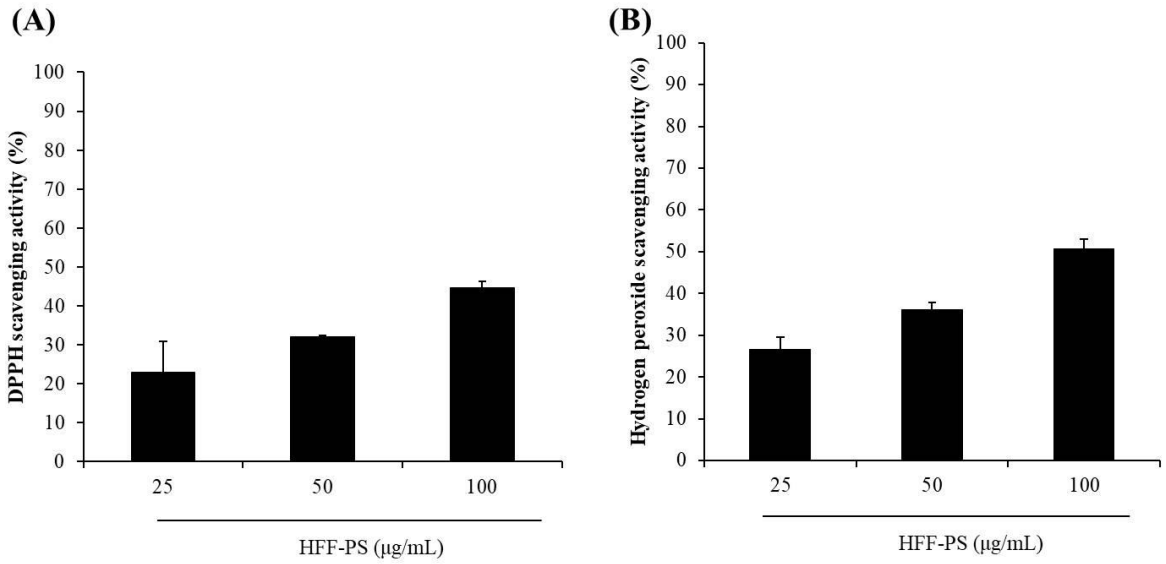

Fig. 13. (A) DPPH radical and (B) hydrogen peroxide scavenging activities of HFF-PS.

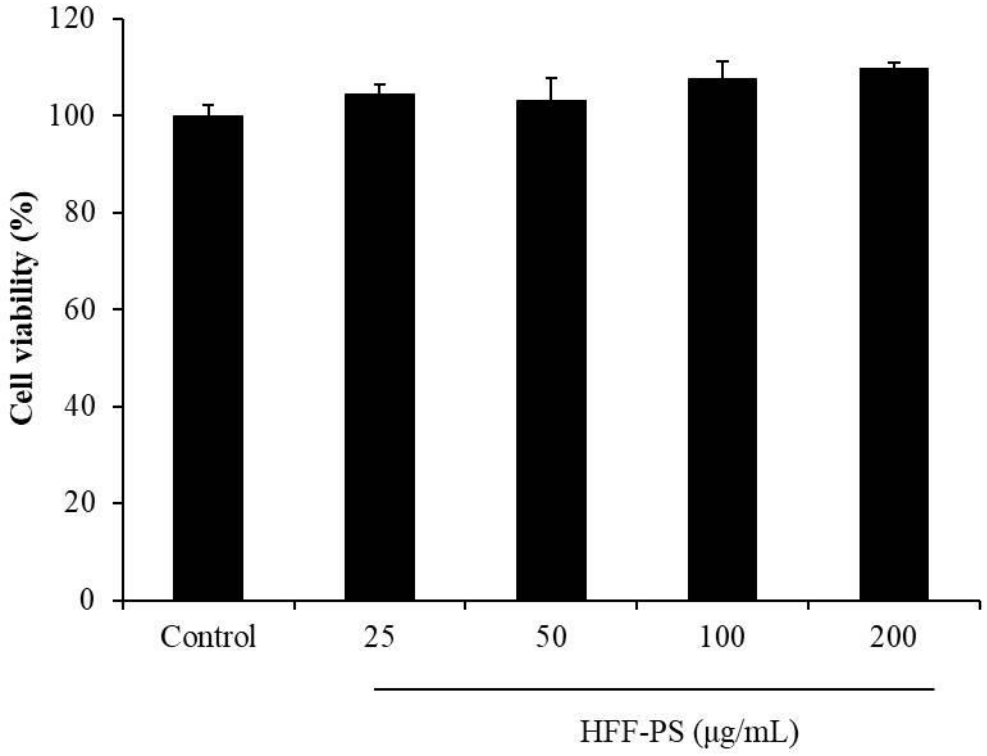

Fig. 14. Cytotoxicity of HFF-PS on Vero cells. Cell viability was measured by MTT assay. The experiments were conducted in triplicate, and the data are expressed as the mean ±SE.

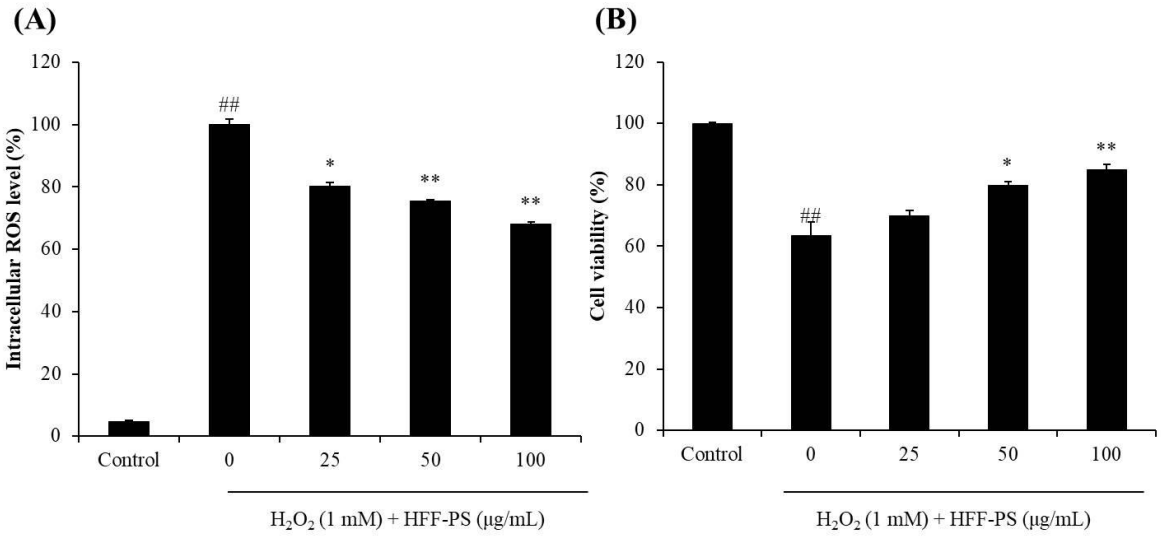

Fig. 15. The intracellular ROS scavenging effect of HFF-PS during H_2O_2-induced oxidative stress in Vero cells (A) and the protective effect of HFF-PS against H_2O_2-induced cell death in Vero cells (B). The experiments were conducted in triplicate, and the data are expressed as the mean ± SE. *$p < 0.05$, ** $p < 0.01$ as compared to the H_2O_2-treated group and $^{\#\#}p < 0.01$ as compared to the control group.

2.4. The effect of HFF-PS on LPS-induced NO generation and cytotoxicity in RAW 264.7 macrophages

The effect of HFF-PS on NO generation and cytotoxicity were measured in LPS-induced RAW 264.7 macrophages. As shown in Fig. 16, HFF-PS significant inhibits NO generation in LPS-induced RAW 264.7 cells (Fig. 16A). In addition, HFF-PS remarket improves cell viability (Fig. 16B). Both effects were dose-dependent. These results displayed that HFF-PS possess strong anti-inflammatory effect in LPS-induced RAW 264.7 cells.

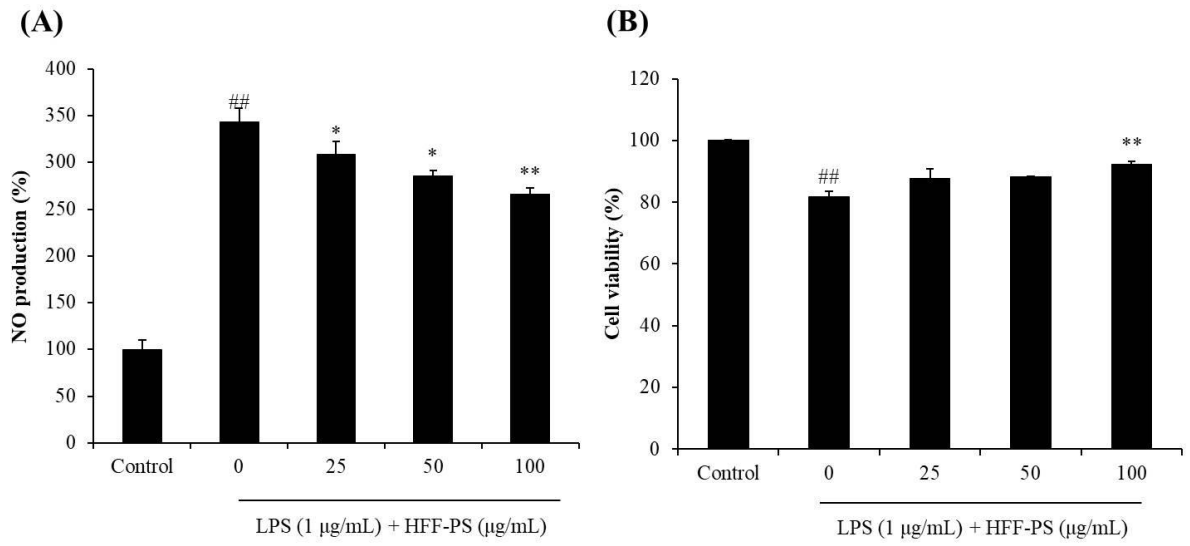

Fig. 16. The effect of HFF-PS on LPS-induced NO generation and cytotoxicity in RAW 264.7 macrophages. (A) NO production in LPS-induced RAW 264.7 macrophages and (B) Cell viability in LPS-induced RAW 264.7 macrophages. The experiments were conducted in triplicate, and the data are expressed as the mean ± SE. *$p < 0.05$, ** $p < 0.01$ as compared to the LPS-treated group and $^{\#\#}p < 0.01$ as compared to the control group.

2.5. Total carbohydrate, phenolic, and sulfate content of fractions separated from HFF-PS

HFF-PS was loaded to a DEAE-cellulose column and eluted by NaCl containing sodium acetate (50 mM, pH 5.0). Five fractions were obtained and named as HFF-PS-F1, HFF-PS-F2, HFF-PS-F3, HFF-PS-F4, and HFF-PS-F5, respectively. The component contents of fractions from HFF-PS were investigated. The phenolic content of fractions from HFF-PS is range from 0.00±0.12% to and 0.27±0.08%, respectively (Table 10). The carbohydrate content of fractions from HFF-PS is range from 25.22±0.91% and 72.06±0.91%. The sulfate content of fractions from HFF-PS is range from 0.00±0.03% and 19.62±0.75%, respectively. HFF-PS-F5 contains a higher carbohydrate content (72.06±0.91%) and sulfate content (19.62±0.75%) than other fractions. Altogether, HFF-PS-F5 contains 91.68% sulfated polysaccharide and thought as a purified fucoidan.

2.6. Monosaccharide composition of fractions separated from HFF-PS

The monosaccharide content of fractions from HFF-PS was determined, using six monosaccharides as standards: fucose, arabinose, rhamnose, galactose, glucose, and xylose. The Table 10 indicated that HFF-PS-F5 comprised by fucose (53.84%), galactose (19.08%), glucose (2.22), and mannose (24.86%).

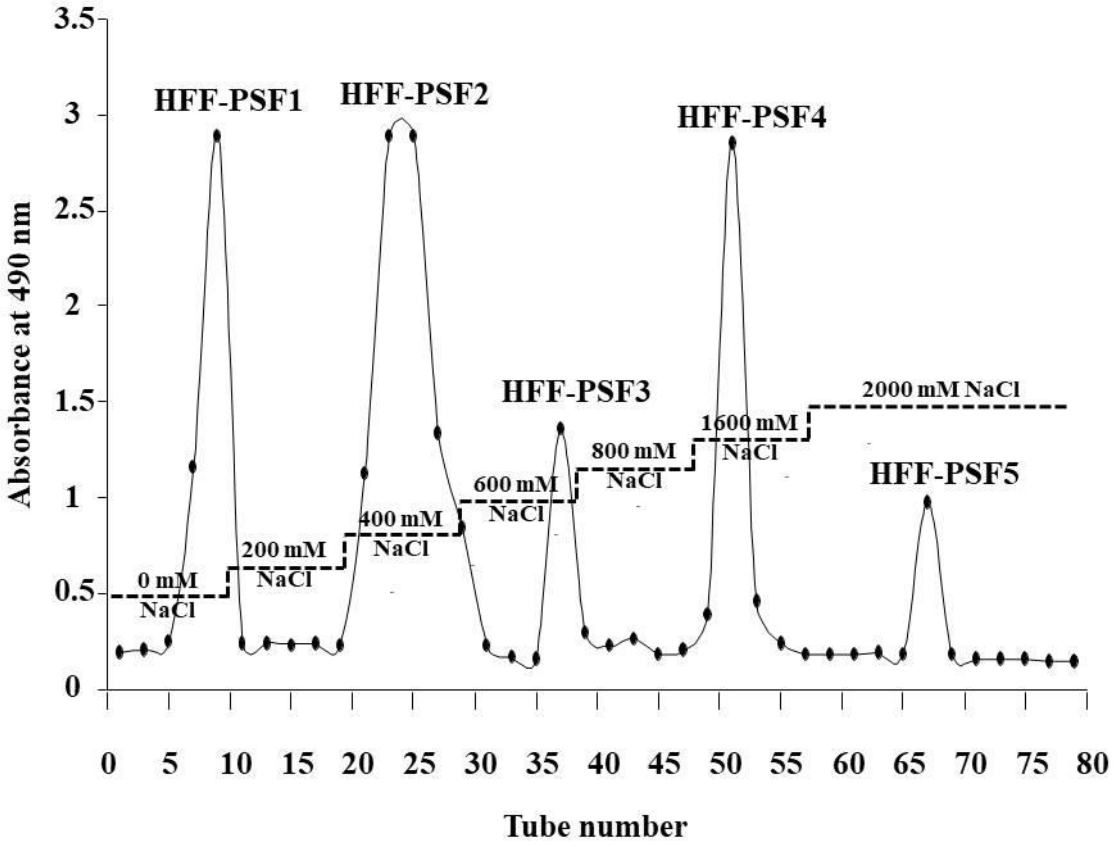

Fig. 17. DEAE-cellulose chromatogram of the polysaccharides separated from HFF-PS.

Table 10. Chemical composition of polysaccharides isolated from HFF-PS by DEAE-cellulose column.

Composition (%)	HFF-PS	F1	F2	F3	F4	F5
Phenolic content	0.00 ±0.15	0.27 ±0.08	0.00 ±0.19	0.00 ±0.19	0.00 ±0.12	0.00 ±0.25
Carbohydrate content	60.63 ±3.04	25.22 ±0.91	25.97 ±0.15	49.15 ±2.58	67.93 ±0.91	72.06 ±0.91
Sulfate content	17.18 ±0.31	0.00 ±1.25	0.00 ±0.07	0.00 ±0.03	11.74 ±0.34	19.62 ±0.75
Sulfated polysaccharide	77.81	25.22	25.97	49.15	79.67	91.68
Monosaccharide content						
Fucose	10.28	25.13	21.73	34.65	52.97	53.84
Galactose	4.65	10.27	20.7	21.85	7.52	19.08
Glucose	80.52	34.35	28.9	18.03	2.15	2.22
Mannose	4.56	30.26	28.67	25.47	37.36	24.86

2.7. DPPH radical and hydrogen peroxide scavenging activity of fractions separated from HFF-PS

Antioxidant activities of fractions separation from HFF-PS has evaluated by investigating the DPPH radical and hydrogen peroxide scavenging activities. As the results shown, all fractions isolated from HFF-PS have shown strong DPPH radical scavenging activity, as well as hydrogen peroxide scavenging activity (Fig. 18 A and B). And HFF-PS-F5 has shown the stronger activity than other fractions for both DPPH radical and hydrogen peroxide. Thus, HFF-PS-F5 has been selected as the target fraction to further studies.

2.8. FT-IR analysis of HFF-PS-F5

To investigate the structural characteristics of HFF-PS-F5, FT-IR ^{1}H NMR spectra of HFF-PS-F5 was determined. The FT-IR spectra of HFF-PS-F5 and commercial fucoidan are shown in Fig. 19. The peaks between 1135 and 1272 cm^{-1} indicate the sulfate groups (S=O stretching) branching off from fucoidan backbone; the absorption at 846 cm^{-1} indicate a sulfate group at axial C-4 [52]. This result indicated that HFF-PS-F5 contains sulfate group in the structure. Thus, we further confirm HFF-PS-F5 is a fucoidan.

2.9. Molecular weight analysis of HFF-PS-F5

The molecular weight of HFF-PS-F5 was determined via HPGPC (Fig. 20). The results indicate that the average molecular weight of HFF-PS-F5 is 231.33 kDa. Thus, according to the about results, HFF-PS-F5 has been identified as a fucoidan with an average molecular weight as 213.33 kDa, which comprised fucose (53.84%), galactose (19.08%), glucose (2.22%), and mannose (24.86%).

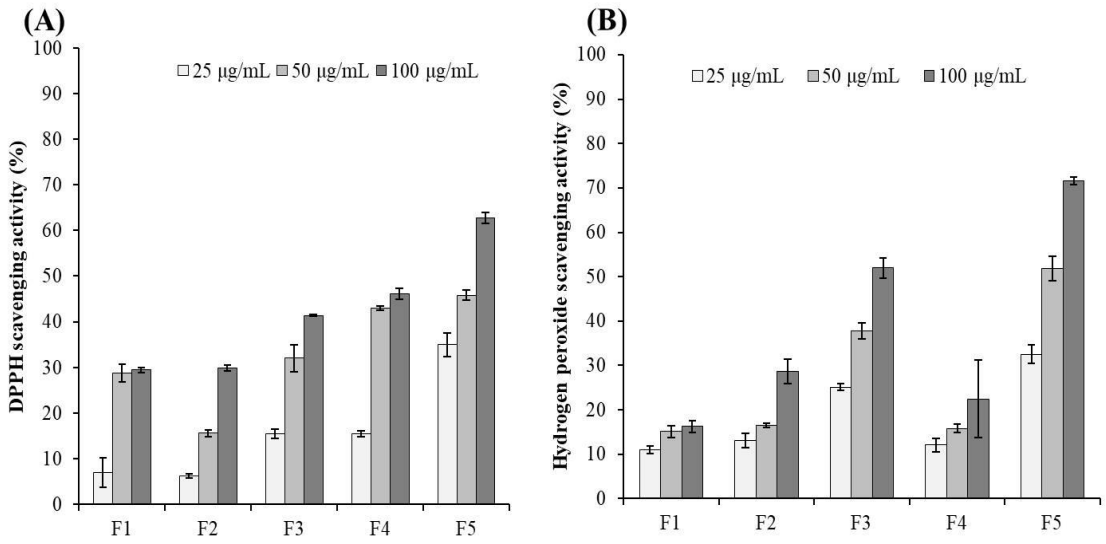

Fig. 18. (A) DPPH radical and (B) hydrogen peroxide scavenging activities of polysaccharides isolated from HFF-PS.

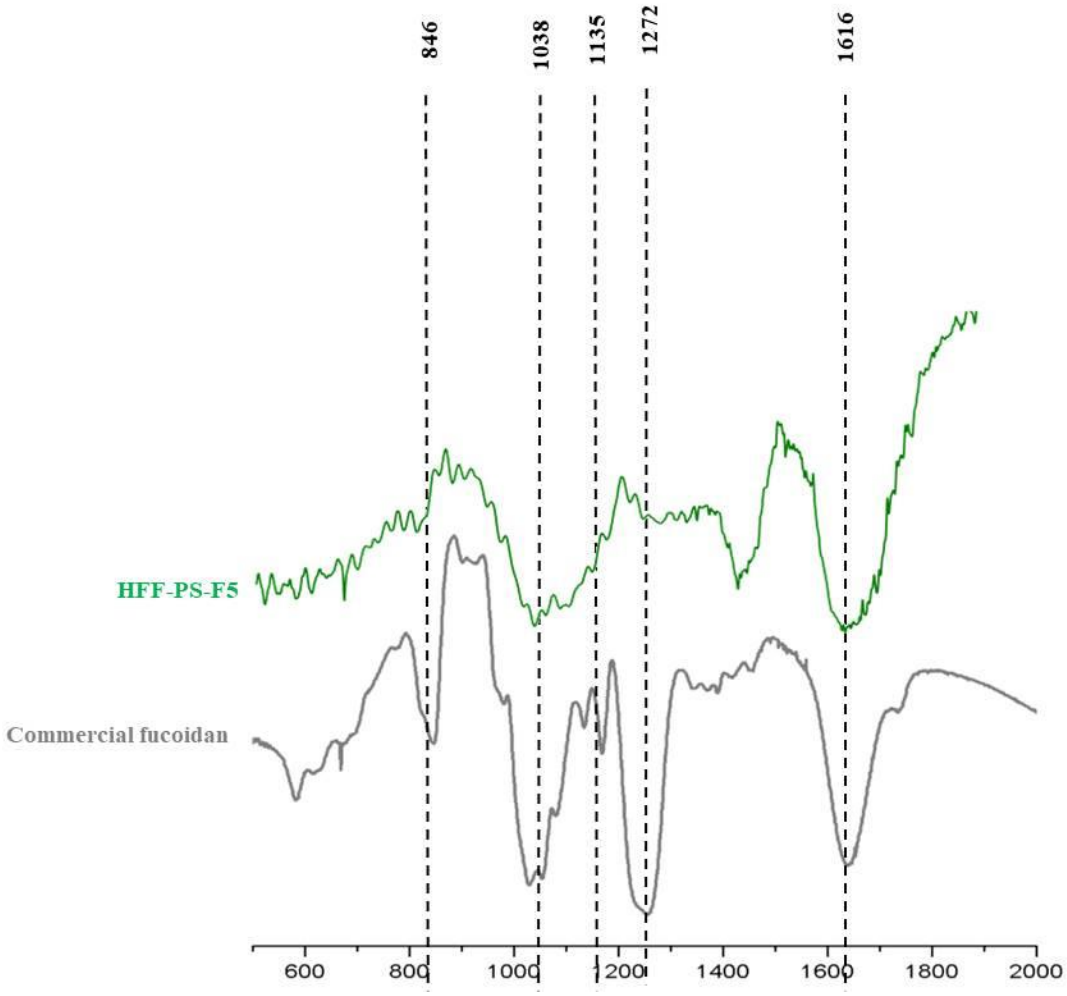

Fig. 19. FT-IR spectra of HFF-PF-F5 and commercial fucoidan.

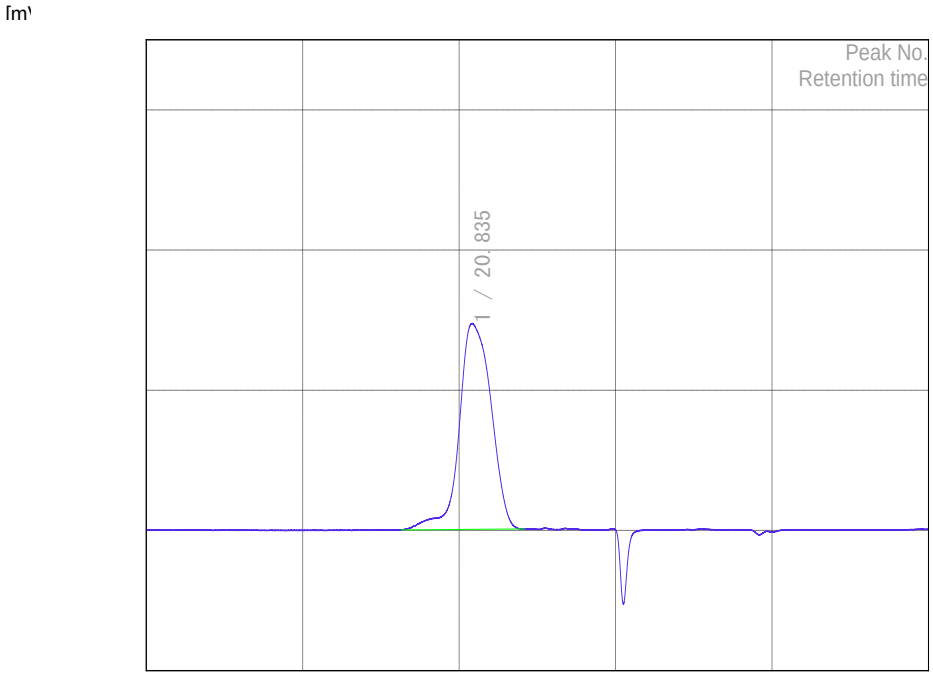

Fig. 20. Gel permeation chromatogram of HFF-PS-F5.

3. Summary

A fucoidan (HFF-PS-F5) was separated from the crude polysaccharides (HFF-PS) from fermented *H. fusiforme*. HFF-PS-F5 contains 91.68% sulfated polysaccharides, which comprise fucose (53.84%), galactose (19.08%), glucose (2.22%), and mannose (24.86%). In addition, the characteristics of HFF-PS-F5 had been determined by Fourier-transform infrared (FT-IR) and HPGPC. The results indicated that HFF-PS-F5 is the fucoidan with an average molecular weight as 213.33 kDa. In the further study, the bioactivities of HFF-PS-F5 have to be further investigated.

Part IV.

Bioactivities of fucoidan isolated from fermented H. fusiforme in in vitro and in vivo models

Section 1: Antioxidant activity of HFF-PS-F5 in vitro in Vero cells and in vivo in zebrafish

Abstract

Protective effect of the fucoidan (HFF-PS-F5) isolated from HFF-PS against hydrogen peroxide (H_2O_2)-induced oxidative stress *in vitro* in Vero cells and *in vivo* in zebrafish had been investigated. HFF-PS-F5 significantly reduced cytotoxicity induced by H_2O_2 in Vero cells. In addition, HFF-PS-F5 reduced intracellular ROS level and apoptosis body formation induced by H_2O_2. The Western blot results demonstrate that HFF-PS-F5 against oxidative stress by improving the expression of endogenous antioxidant enzymes including catalase and superoxidase dismutase (SOD) via regulating Nrf2 pathways. In addition, HFF-PS-F5 has strongly protective against H_2O_2-stimulated oxidative stress *in vivo* zebrafish that demonstrated in improving survival rate, decreasing heart beating rate, and reducing ROS generation, cell death and lipid peroxidation. These results suggest that HFF-PS-F5 may use as a beneficial antioxidant ingredient in medical and cosmetic industries.

1. Materials and methods

1.1. Chemicals and reagents

3-(4,5-dimethylthiazol-2-yl)-2,5-diphenyltetrazolium bromide (MTT), dimethyl sulfoxide (DMSO), acridine orange, and 2,7-dichlorofluorescein diacetate (DCFH-DA) were purchased from SIGMA-ALDRICH (St. Louis, MO, USA). Roswell Park Memorial Institute-1640 (RPMI-1640) medium, trypsin-EDTA, penicillin-streptomycin, and fetal bovine serum (FBS) were purchased from Gibco-BRL (Grand Island, NY, USA). Catalase, superoxidase dismutase (SOD),β-actin, and nuclear factor (erythroid-derived 2)-like 2 (Nrf2) antibodies, anti-mouse and anti-rabbit IgG antibodies were purchased from Cell Signaling Technology (Beverly, MA, USA).All other chemicals and reagents were analytical grade.

1.2. Cell culture

The monkey kidney fibroblasts (Vero cells) were purchased from the Korea Cell Line Bank (KCLB, Seoul, Korea). Cells were maintained in RPMI-1640 medium containing 10% heat-inactivated FBS, penicillin (100 unit/mL), and streptomycin (100 μg/mL) at 37 °C under humidified atmosphere containing 5% CO_2. Cells were sub-cultured every 3 days and seeded at a concentration of 1×10^5 cells/mL for experiments.

1.3. Determination of the protective effect of HFF-PS-F5 against H_2O_2-induced intracellular ROS generation in Vero cells

To measure the intracellular ROS levels of H_2O_2-stimulated Vero cells, Vero cells were seeded in a 24-well plate and incubated for 24 h. Cells were treated with different concentrations (25, 50, and 100 μg/mL) of HFF-PS-F5 and incubated for 1h. After incubation, H_2O_2 (1 mM) was added to the wells, followed by incubation for 1h. Finally, the intracellular ROS levels were measured by the DCF-DA assay [71].

1.4. Measurement of the protective effect of HFF-PSF5 against H_2O_2-induced cytotoxicity in Vero cells

Vero cells were treated with different concentrations of HFF-PS-F5 and incubated for 1 h. After incubation, H_2O_2 (1 mM) was added to the cells prior to incubation for 24 h. Cell viability was measured by MTT assay, according to Fernando et al. [18].

1.5. Nuclear staining with Hoechst 33342

To assess the apoptosis body's formation in H_2O_2-induced Vero cells, the nuclear morphology of cells was analyzed by Hoechst 33342 staining. Nuclear staining was performed base on the method described by Wijesinghe et al. [72]. The degree of nuclear condensation of cells was examined under a fluorescence microscope equipped with a Cool SNAP-Pro color digital camera (Olympus, Japan).

1.6. Western blot analysis

The effect of HFF-PS-F5 on the expressions of catalase, SOD, and Nrf2, was assessed by Western blot analysis performed as described previously. In brief, cells were treated with HFF-PS-F5 and stimulated with H_2O_2. After 24 h incubation, cells were harvested. Proteins were extracted with the PROPREP protein extraction kit (iNtRON Biotechnology, Sungnam, Korea). The protein level of each sample was measured by a BCA^{TM} kit. Total proteins (50 μg) were separated on 12% SDS-polyacrylamide gels and transferred to pure nitrocellulose membranes. Membranes were blocked with 5% skim milk for 3 h at room temperature and incubated with primary antibodies overnight at 4℃. After washing with TBS-T buffer, membranes were incubated with secondary antibodies for 3 h at room temperature. Finally, the protein bands were visualized using an ECL western blotting detection kit and exposed on X-ray films.

1.7. Origin and maintenance of zebrafish

The adult zebrafish were purchased from a commercial market (Seoul Aquarium, Korea) and 10 fishes were kept in a 3 L acrylic tank under the condition as followed: 28.5℃, in 14/10 h light/dark cycle. The fish were fed with Tetramin flake feed supplemented with live brine shrimp (Artemia salina) three times per day, 6 days a week. Embryos were collected from natural spawning that was induced by turn on the light in the morning, and the collection of embryos was completed within 30 min.

1.8. Application of HFF-PS-F5 and H_2O_2 to zebrafish embryos

Approximately 3-4 h post-fertilization (hpf), the embryos were transferred to a 12-well plate (15 embryos per well) and incubated in embryo medium containing HFF-PS-F5 (25, 50, and 100 μg/mL). After 1 h incubation, H_2O_2 (10 mM) was added to each well, then, the embryos were incubated with H_2O_2 until 24 hpf. The survival rate of zebrafish was measured at 3 days post-fertilization (dpf) by counting the live fish, and the surviving fish were used for further analysis.

1.9. Measurement of heart-beating rate, ROS generation, cell death, and lipid peroxidation in zebrafish

The heart-beating rate of zebrafish was measured base on the protocol described by Sanjeewa et al. [52]. Intracellular ROS generation, cell death, and lipid peroxidation were measured in live zebrafish using DCFH-DA, acridine orange, and DPPP staining at 3 dpf, respectively, according to Kang et al. [73]. The anesthetized zebrafish were photographed under a fluorescence microscope equipped with a Cool SNAP-Pro color digital camera (Olympus, Japan) and the fluorescence intensity of individual zebrafish was quantified using the Image J program.

1.10. Statistical analysis

All the experiments were performed in triplicate. The data were expressed as the mean ± standard error (SE), and one-way ANOVA test (using SPSS 12.0 statistical software) was used to statistically compare the mean values of each treatment. Significant differences between the means of parameters were determined by Duncan's multiple range tests, $p < 0.05$ and $p < 0.01$ were considered as significantly different.

2. Results and discussion

2.1. Protective effect of HFF-PS-F5 against H_2O_2-induced oxidative stress in Vero cells

As shown in Fig. 21, the intracellular ROS level significantly increased and cell viability decreased following treatment with H_2O_2. However, the intracellular ROS levels decreased and cell viability increased following treatment at all measured concentrations of HFF-PS-F5. These results indicated that HFF-PS-F5 effectively protect Vero cells against oxidative stress induced by H_2O_2.

2.2. Protective effect of HFF-PS-F5 against H_2O_2-induced apoptosis

In order to measure the apoptotic body formation stimulated by H_2O_2, Vero cells were stained with Hoechst 33342 and visualized by fluorescent microscopy. As Fig. 22 shows, there were significantly apoptotic bodies formed in the cells treated with H_2O_2. However, the amounts of apoptotic bodies in cells that pre-treated with different concentrations of HFF-PS-F5 were significantly decreased in a dose-dependent manner. This result suggested that HFF-PS-F5 effectively against apoptosis in H_2O_2-induced Vero cells.

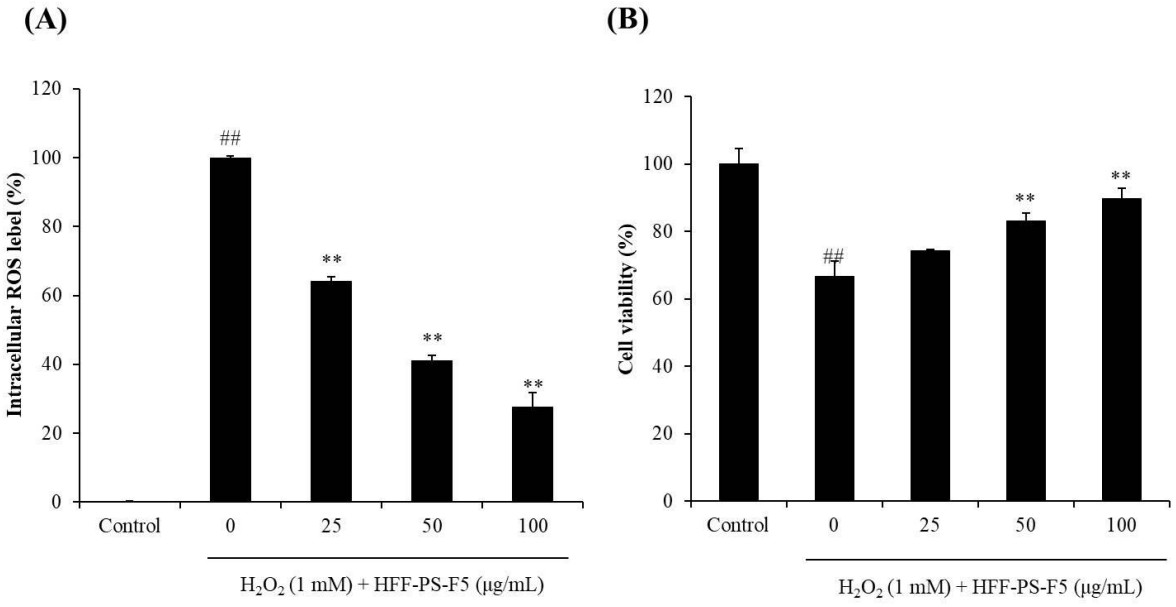

Fig. 21. The intracellular ROS scavenging effect of HFF-PS-F5 during H_2O_2-induced oxidative stress in Vero cells (A) and the protective effect of HFF-PS-F5 against H_2O_2-induced cell death in Vero cells (B). The experiments were conducted in triplicate, and the data are expressed as the mean ± SE. ** $p < 0.01$ as compared to the H_2O_2-treated group and $^{\#\#}p < 0.01$ as compared to the control group.

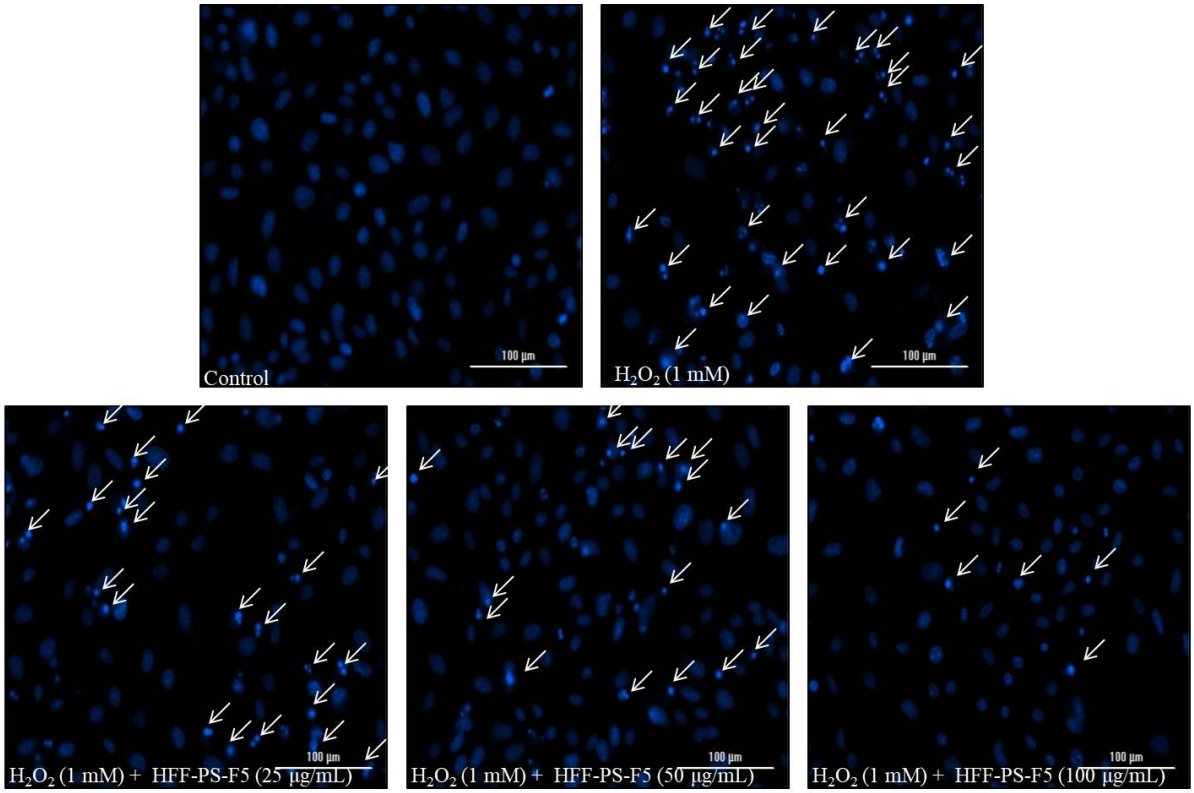

Fig. 22. The protective effect of HFF-PS-F5 against H_2O_2-induced apoptosis in Vero cells. The apoptotic body formation was observed under a fluorescence microscope after Hoechst 33342 staining.

2.3. HFF-PS-F5 improves the expression of catalase and SOD via regulating Nrf2 pathway in H_2O_2-induced Vero cells

Normally, Nrf2 located in the cytosol and bound to a control protein that Kelch-like ECH-associated protein 1 (Keap1). In the oxidative stress condition, Nrf2 is parted from Keap1, initiates translocation to the nucleus, and active the antioxidant genes to expression antioxidant enzymes such as catalase and SOD [74, 75]. As Fig. 23A shows, H_2O_2 significantly reduced catalase and SOD levels. However, HFF-PS-F5 remarkably increased the catalase and SOD levels in H_2O_2-stimulated Vero cells (Fig. 23A). Further results indicated that HFF-PS-F5 stimulated total Nrf2 level in H_2O_2-stimulated Vero cells (Fig. 23B). These results demonstrate that HFF-PS-F5 possesses the protective effect against oxidative stress induced by H_2O_2 through production of antioxidant enzymes including catalase and SOD via regulating the Nrf2 pathway.

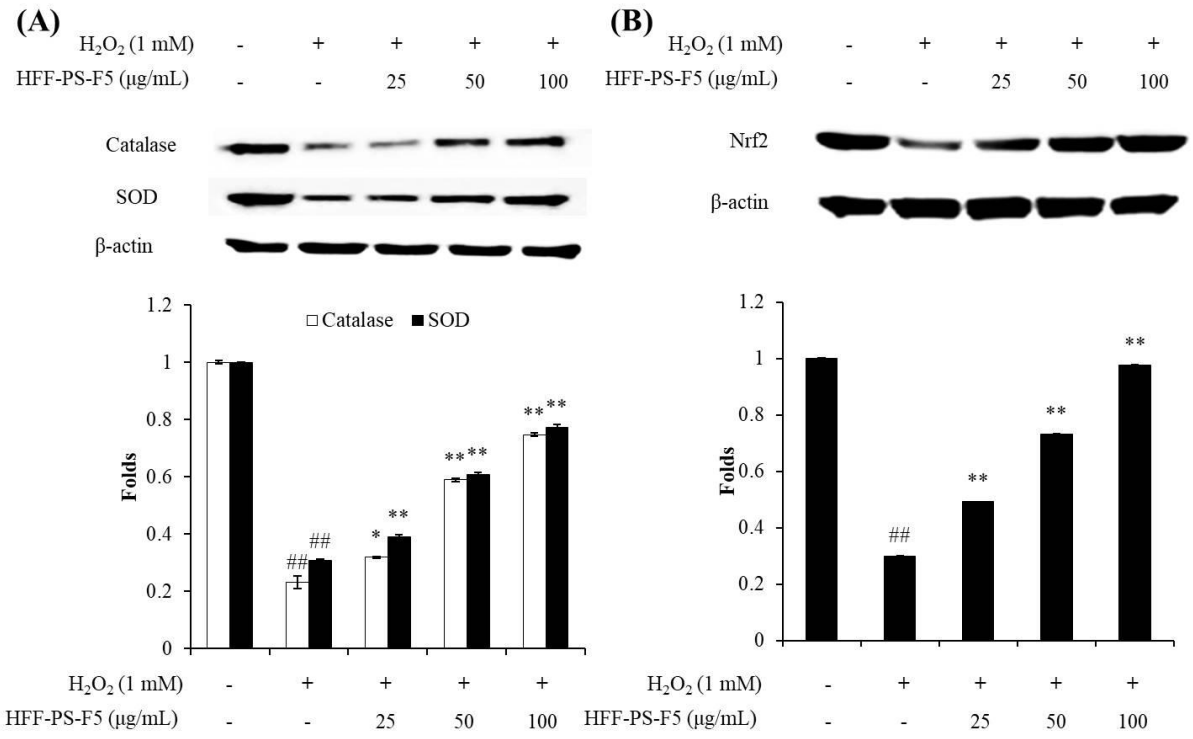

Fig. 23. The effect of HFF-PS-F5 on Nrf2 pathway and antioxidant enzymes expression in H_2O_2-stimulated Vero cells. (A) The expression of Catalase and SOD; (B) the expression of Nrf2. $^{*}p < 0.05$, $^{**}p < 0.01$ as compared to the H_2O_2-treated group and $^{\#\#}p < 0.01$ as compared to the control group.

2.4. HFF-PS-F5 improves survival rate and reduces heart-beating rate in H_2O_2-induced zebrafish

Zebrafish is a popular animal model in toxicological and pharmacological studies, especially in chemical toxicity and drug discovery. Our previous studies indicated that H_2O_2 significantly induced oxidative stress in zebrafish demonstrate in decreasing survival rate and increasing the heart-beating rate as well as inducing ROS production, cell death, and lipid peroxidation [76].

The survival rates and heart-beating rates of H_2O_2-treated zebrafish were measured. The survival rate and heart-beating rate of zebrafish that did not treat with H_2O_2 were considered to be 100% (Fig. 24). The survival rate of zebrafish treated with H_2O_2 was significantly decreased (Fig. 24A). However, the survival rates of HFF-PS-F5-treated zebrafish were significantly increased. The heart-beating rate of the zebrafish treated with H_2O_2 was 109% (Fig. 24B), but significantly decreased with HFF-PS-F5 treatment.

2.5. Protective effect of HFF-PS-F5 against H_2O_2-induced ROS generation, cell death, and lipid peroxidation in zebrafish

The effect of HFF-PS-F5 on ROS generation in H_2O_2-treated zebrafish was measured by detection of DCF-DA. As Fig. 25 shows, HFF-PS-F5 significantly decreased ROS levels in a dose-dependent manner. In addition, the cell death was significantly increased in the zebrafish treated with H_2O_2; however, it is remarkably and dose-dependently decreased in the zebrafish treated with different concentrations of HFF-PS-F5 (Fig. 26). Furthermore, HFF-PS-F5 effectively protected against H_2O_2-induced lipid peroxidation in zebrafish (Fig. 27).

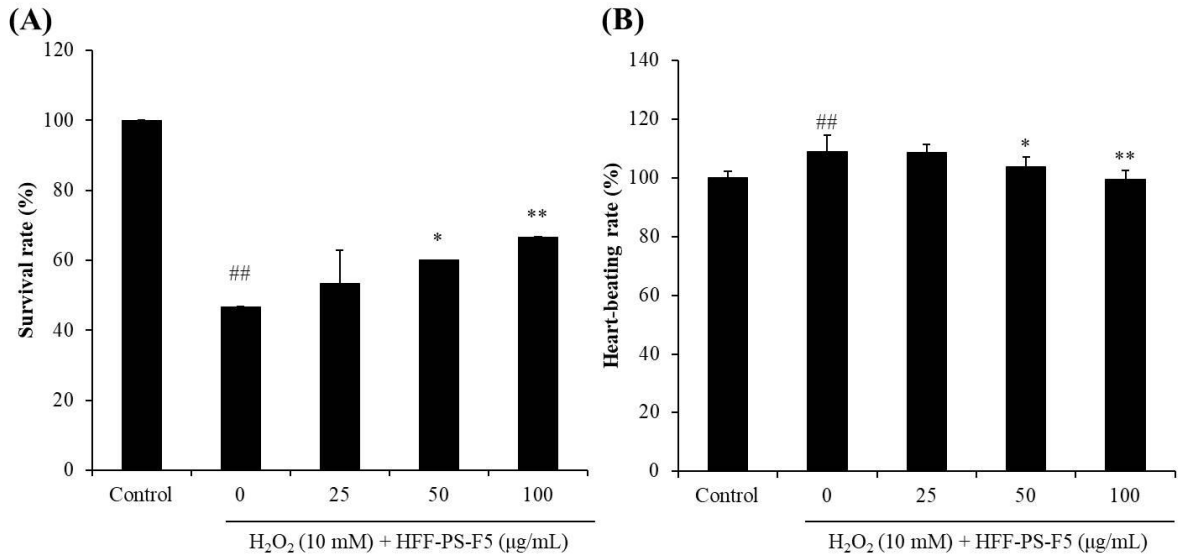

Fig. 24. The survival rate and heart-beating rate of zebrafish after pretreatment with HFF-PS-F5 and/or treatment with H_2O_2. (A) Survival rate; (B) heart-beating rate. The experiments were conducted in triplicate, and the data are expressed as the mean ± SE. *$p < 0.05$, ** $p < 0.01$ as compared to the H_2O_2-treated group and $^{\#\#}p < 0.01$ as compared to the control group.

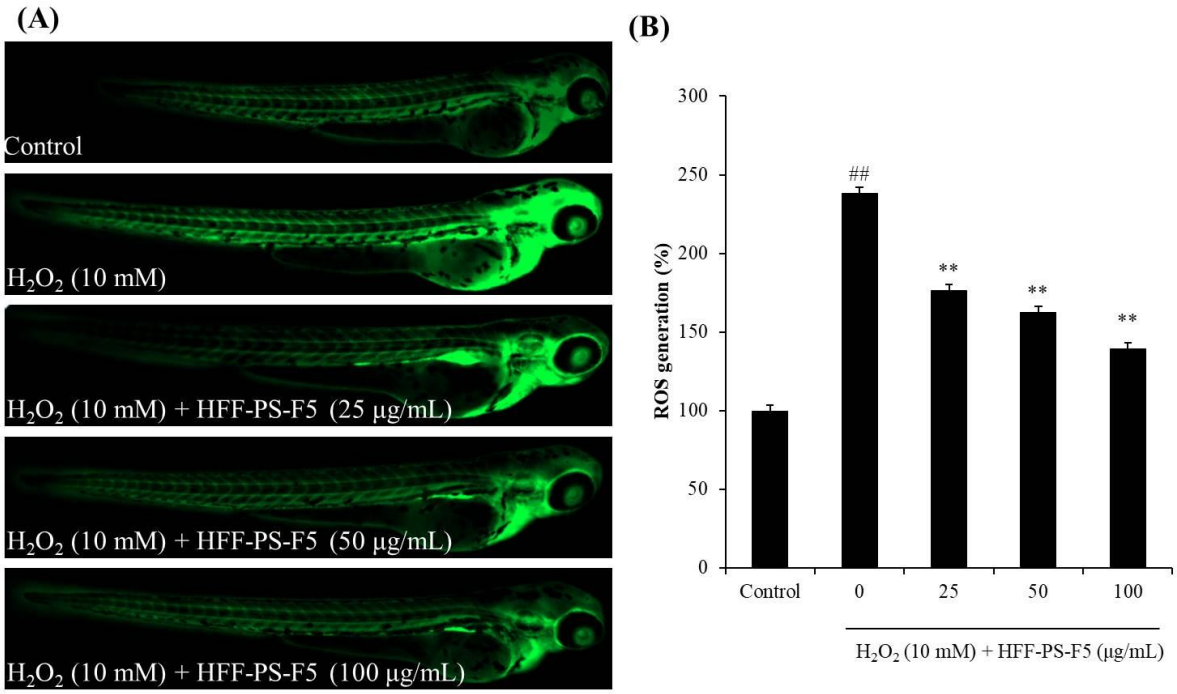

Fig. 25. The protective effect of HFF-PS-F5 during H_2O_2-induced ROS production in zebrafish embryos. (A) Zebrafish embryo under fluorescence microscope; (B) the levels of ROS generation. ROS levels were measured using Image J software. The experiments were conducted in triplicate, and the data are expressed as the mean ± SE. *$p < 0.05$, ** $p < 0.01$ as compared to the H_2O_2-treated group and $^{\#\#}p < 0.01$ as compared to the control group.

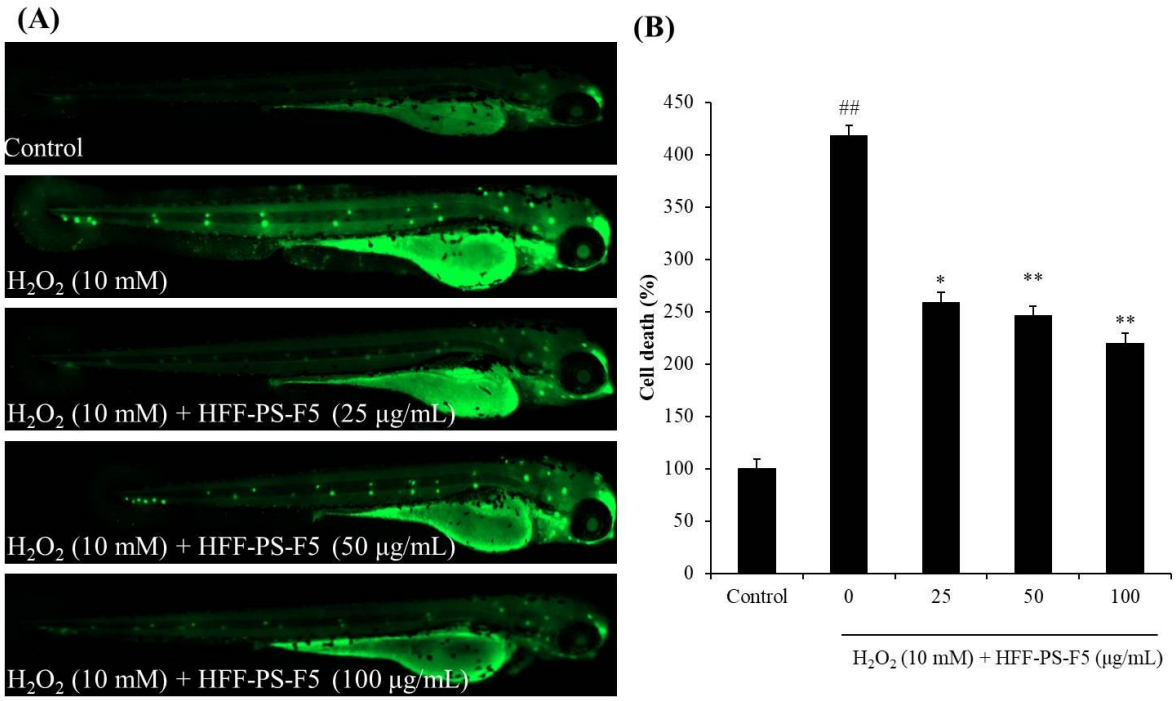

Fig. 26. The protective effect of HFF-PS-F5 during H_2O_2-induced cell death in zebrafish embryos. (A) Zebrafish embryo under fluorescence microscope; (B) the measured levels of cell death. Cell death levels were measured using Image J software. The experiments were conducted in triplicate, and the data are expressed as the mean ± SE. *$p < 0.05$, ** $p < 0.01$ as compared to the H_2O_2-treated group and $^{\#\#}p < 0.01$ as compared to the control group.

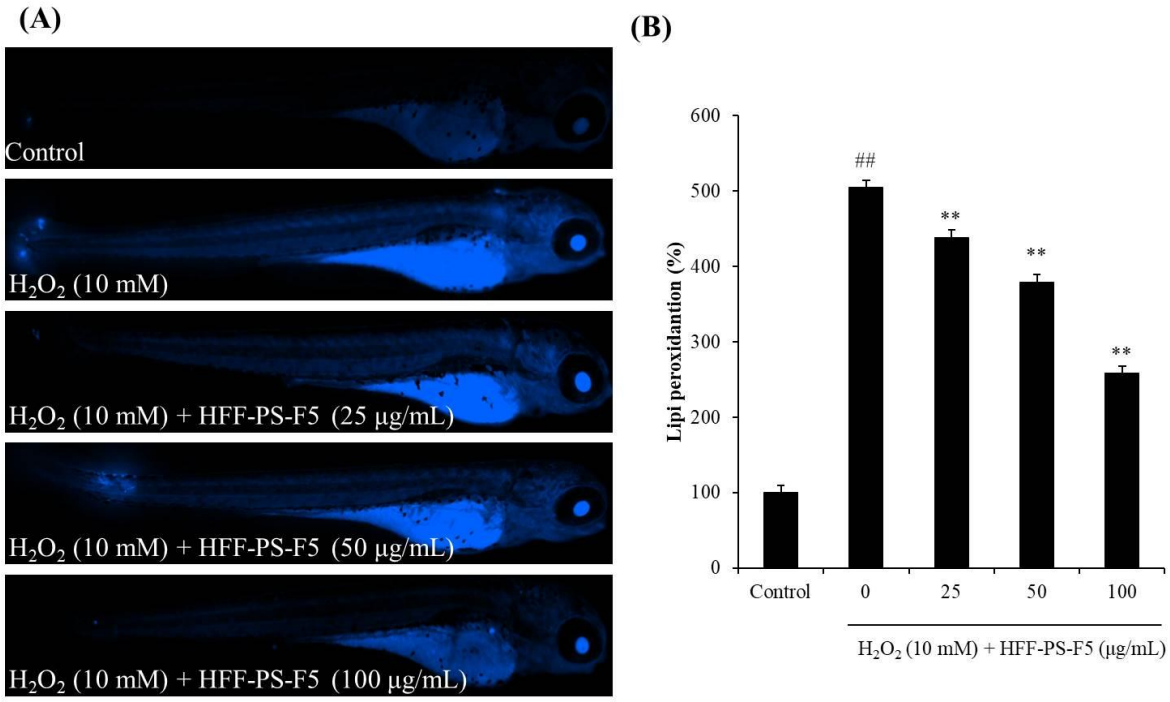

Fig. 27. The protective effect of HFF-PS-F5 during H_2O_2-induced lipid peroxidation in zebrafish embryos. (A) Zebrafish embryo under fluorescence microscope; (B) the measured levels of cell death. Cell death levels were measured using Image J software. The experiments were conducted in triplicate, and the data are expressed as the mean ± SE. *$p < 0.05$, ** $p < 0.01$ as compared to the H_2O_2-treated group and $^{\#\#}p < 0.01$ as compared to the control group.

3. Summary

In summary, HFF-PS-F5 possesses strong *in vitro* antioxidant activity demonstrate in reducing intracellular ROS and improving cell viability in H_2O_2-stimulated Vero cells. In addition, it possesses strong *in vivo* antioxidant activity demonstrated in improving the survival rate, decreasing heart-beating rate, and reducing ROS generation and cell death in H_2O_2-stimulated zebrafish. These results suggest that HFF-PS-F5 could consider for use in the medical and cosmetic industries.

Section 2: Anti-inflammatory effect of HFF-PS-F5 *in vitro* in RAW 264.7 macrophages and *in vivo* in zebrafish

Abstract

In the present study, the anti-inflammatory effect of the fucoidan (HFF-PS-F5) isolated from HFF-PS was investigated *in vitro* in RAW 264.7 macrophages and *in vivo* in zebrafish. The results indicated that HFF-PS-F5 significantly inhibited NO generation stimulated by LPS in RAW 264.7 cells. In addition, HFF-PS-F5 dose-dependently improved the cell viability in LPS-stimulated RAW 264.7 cells. Moreover, HFF-PS-F5 significantly decreased the expression of tumor necrosis factor alpha (TNF-α), prostaglandin E_2 (PGE_2), interleukin-1 beta (IL-1β), and interleukin-6 (IL-6). Furthermore, HFF-PS-F5 suppressed the expression of inducible nitric oxide synthase (iNOS) and cyclooxygenase-2 (COX-2) by regulating the nuclear factor kappa-B (NF-κB) pathway. The *in vivo* test results suggested HFF-PS-F5 significantly reduced ROS, cell death, and NO levels in LPS-stimulated zebrafish. These results demonstrate that HFF-PS-F5 possesses strong *in vitro* and *in vivo* anti-inflammatory activities and could be potentially used as an ingredient to developing anti-inflammatory agent or cosmetic.

1. Materials and methods

1.1. Reagents and chemicals

Lipopolysaccharides (LPS), acridine orange, DCFH-DA, DMSO, and DAF-DM-DA were purchased from Sigma-Aldrich (St. louis, MO, USA). Fetal bovine serum (FBS), penicillin–streptomycin (P/S), and Dulbecco's modified Eagle's medium (DMEM) were purchased from Gibco/BRL (Grand Island, NY, USA). The ELISA kits for measuring prostaglandin E_2 (PGE_2), interleukin-6 (IL-6), tumor necrosis factor-α (TNF-α), and interleukin-1β (IL-1β) levels were purchased from R&D Systems Inc (Minneapolis, MN, USA). Antibodies against β-actin, cyclooxygenase 2 (COX-2), nitric oxide synthase (iNOS) IκBα, p-IκBα, p50 NF-κB, p65 NF-κB nucleolin, β-actin, and anti-rabbit antibody antibodies were purchased from Thermo Scientific (Waltham, MA, USA). All other chemicals used in this study were of analytical grade.

1.2. Cell culture

RAW 264.7 macrophages were purchased from ATCC (TIB-71^{TM}). RAW 264.7 cells were grown in DMEM supplemented with 10% FBS, penicillin (100 unit/mL) and streptomycin (100 μg/mL). Cells were maintained at 37℃ in an incubator containing 5% CO_2 and seeded at a concentration of 1×10^5 cells/mL for the experiment.

1.3. Measurement of NO production and cell viability

The experiments were performed following the methods described by Heo et al. [9]. RAW 264.7 cells were seeded in 24-well plates for 24 h. HFF-PS-F5 was added into each well, achieving final concentrations of 25, 50, and 100 μg/mL. After 1 h, LPS (1 μg/mL) was

introduced into all wells, except control. After 24 h, the NO production was measured by Griess assay and cell viability was measured by MTT assay according to the protocol described in the previous study [68, 77, 78].

1.4. Measurement of PGE_2 and pro-inflammatory cytokine (TNF-α, IL-1β, and IL-6) production

The experiments were performed following the methods described by Heo et al. [9]. RAW 264.7 cells were seeded in 24-well plates for 24 h. HFF-PS-F5 was added into each well, achieving final concentrations of 25, 50, and 100 μg/mL. After 1 h, LPS (1 μg/mL) was introduced into all wells, except control. After 24 h, the culture medium was collected and used for measuring PGE_2, TNF-α, IL-6, and IL-1β production levels. The PGE_2, TNF-α, IL-6, and IL-1β production levels were evaluated using the commercial ELISA kits following the manufacturer's instructions. The cell viability was measured by MTT assay base on the method described by Wang et al [47].

1.5. Western blot analysis

RAW 264.7 cells were seeded in 6-well plates. After 24 h, cells were treated with HFF-PS-F5 and exposed to LPS (1 μg/mL) 1 h later. Following a second incubation period of 1 h (for NF-κB analysis) or 24 h (for COX-2 and iNOS analysis), cells was harvested and the proteins were extracted with the PROPREP protein extraction kit (iNtRON Biotechnology, Sungnam, Korea). The protein concentration of each lysate was determined using a BCA™ kit. Each 30 μg of protein were separated on a 12% SDS–polyacrylamide gel, and the protein bands were transferred onto a polyvinylidene fluoride membrane. The membranes were blocked with blocking buffer (5% blotting-grade blocker), and the membrane was then incubated with specific primary antibodies overnight, at 4℃. After incubation, the membranes were washed

with TBS-T buffer and incubated with secondary antibodies at room temperature for 3 h. Finally, the signals were developed by an ECL western blotting detection kit, and exposed on X-ray films.

1.6. Application of HFF-PS-F5 and LPS to zebrafish embryos

Approximately 3~4 hours post-fertilization (hpf), the embryos were transferred to individual wells in a 12-well plate (15 embryos per group) and maintained in embryo medium containing HFF-PF-F5 (25, 50, and 100 μg/mL). After 1 hour incubation, 10 μg/mL LPS was added to the medium, and the embryos were incubated until 24 hpf. The survival rate was measured at 3 days post-fertilization (dpf) after treatment with LPS by counting live embryos, and the surviving fish were then used for further analysis.

1.7. Determination of heart-beating rate, ROS generation, cell death, and NO generation in zebrafish

The zebrafish heart-beating rate was measured according to Sanjeewa et al. [52]. The zebrafish heart-beating rate in both the atrium and ventricle was recorded for 1 min at 2 dpf under a microscope. Intracellular ROS level, cell death, and NO generation were measured in live embryos using DCFH-DA, acridine orange, and DAF-FM-DA staining, respectively, followed the previous procedure [34, 79, 80]. The zebrafish were observed and photographed under a fluorescence microscope equipped with a Cool SNAP-Pro color digital camera (Olympus, Japan). The fluorescence intensity of individual zebrafish larva was quantified using the image J program.

1.8. Statistical analysis

All the experiments were performed in triplicate. The data were expressed as the mean ± standard error (SE), and one-way ANOVA test (using SPSS 12.0 statistical software) was

used to statistically compare the mean values of each treatment. Significant differences between the means of parameters were determined by Duncan's multiple range tests, $p < 0.05$ and $p < 0.01$ were considered as significantly different.

2. Results and discussion

2.1. The effect of HFF-PS-F5 on LPS-induced NO generation and cytotoxicity in RAW 264.7 macrophages

The effect of HFF-PS-F5 on NO generation and cytotoxicity were measured in LPS-induced RAW 264.7 macrophages. As shown in Fig. 28, HFF-PS-F5 significant inhibits NO generation in LPS-induced RAW 264.7 cells. In addition, HFF-PS-F5 remarkable improves cell viability. Both effects were dose-dependent.

2.2. HFF-PS-F5 decreased PGE_2 and pro-inflammatory cytokines release in LPS-induced RAW 264.7 macrophages

As shown in Fig. 29, LPS significant increase in the production of TNF-α, IL-1β, IL-6, and PGE_2 compared with the control. However, the TNF-α, IL-1β, IL-6, and PGE_2 levels in HFF-PS-F5 treated RAW 264.7 cells were significantly decreasing, which was dose-dependent with increasing sample concentrations.

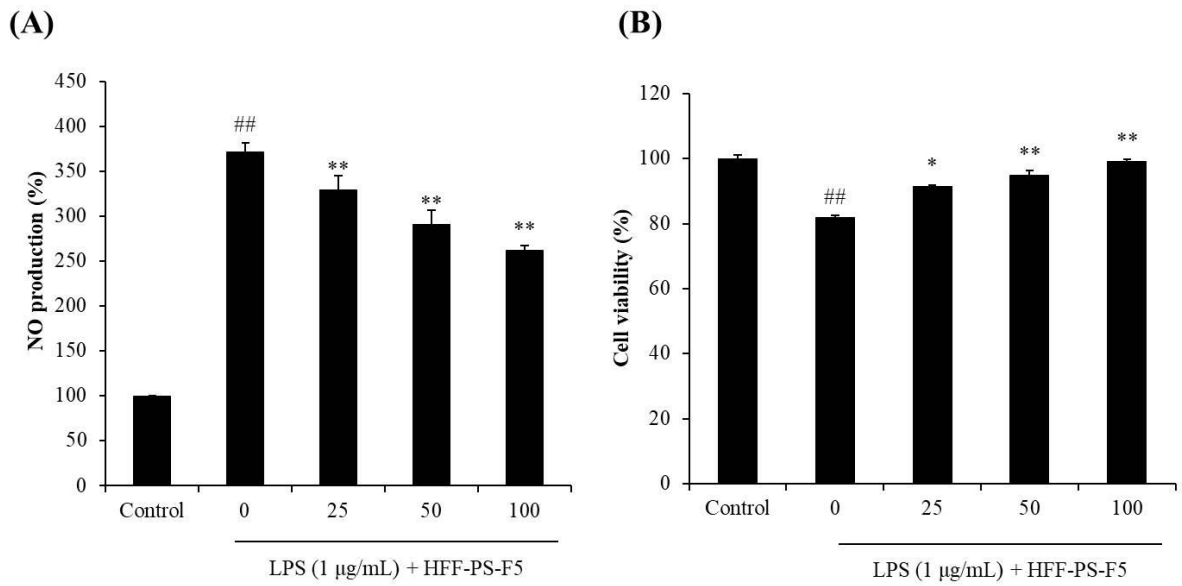

Fig. 28. The effect of HFF-PS-F5 on LPS-induced NO generation and cytotoxicity in RAW 264.7 macrophages. (A) NO production in LPS-induced RAW 264.7 macrophages and (B) Cell viability in LPS-induced RAW 264.7 macrophages. The experiments were conducted in triplicate, and the data are expressed as the mean ± SE. *$p < 0.05$, ** $p < 0.01$ as compared to the LPS-treated group and $^{\#\#}p < 0.01$ as compared to the control group.

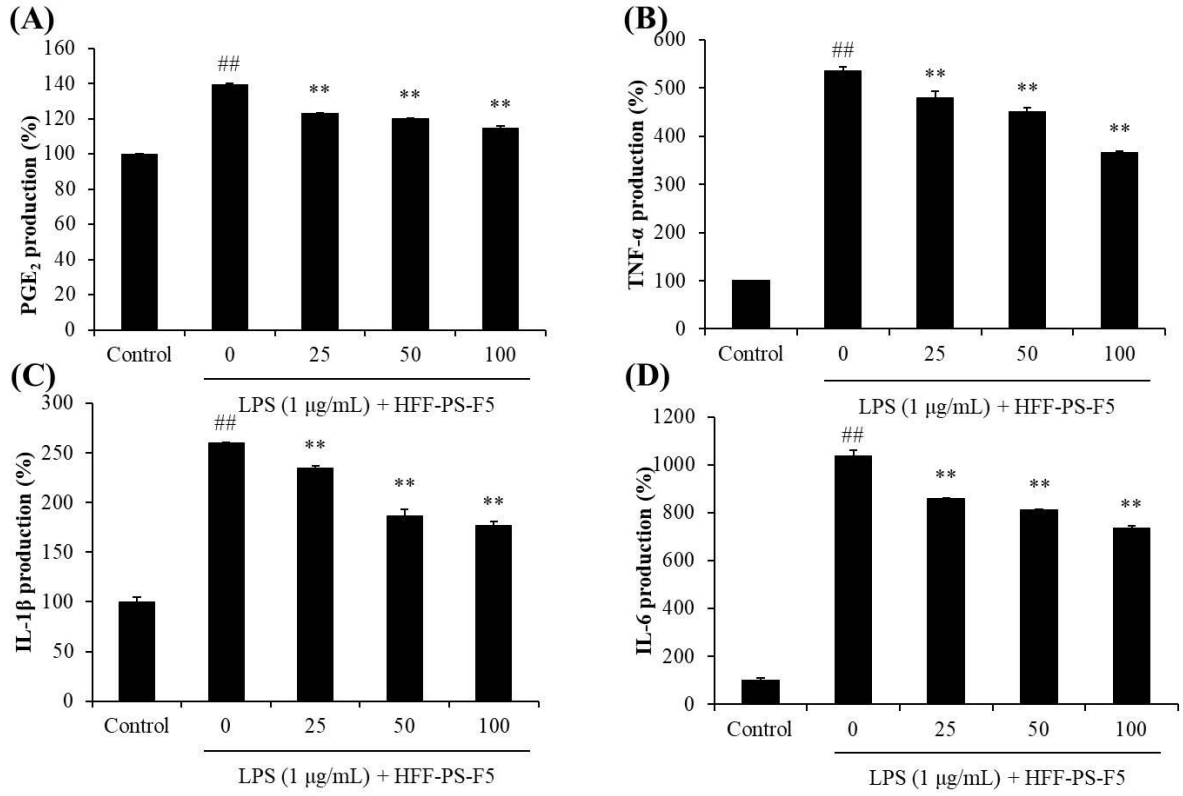

Fig. 29. The inhibitory effect of HFF-PS-F5 upon the production of PGE_2 (A) , TNF-α (B), IL-1β (C) , and IL-6 (D) in LPS-stimulated RAW 264.7 macrophages. The experiments were conducted in triplicate, and the data are expressed as the mean ±SE. ** $p < 0.01$ as compared to the LPS-treated group and $^{\#\#}p < 0.01$ as compared to the control group.

2.3. HFF-PS-F5 inhibited the expression of iNOS and COX-2 in LPS-induced RAW 264.7 macrophages

COX-2 and iNOS are two inducible enzymes, which synthesis the two key inflammatory mediators NO and PGE_2, respectively [81]. The levels of COX-2 and iNOS were up-regulated in inflammatory response [82]. Therefore, we investigated the effect of HFF-PS-F5 on the expression levels of COX-2 and iNOS in LPS-stimulated RAW 264.7 cells. The expression levels of iNOS and COX-2 are shown in Fig. 30. According to the results, the expression levels of iNOS and COX-2 were significantly increased in the cells treated with LPS only. However, HFF-PS-F5 effectively suppressed iNOS and COX-2 expression in a dose-dependent manner. These results indicate that HFF-PS-F5 possesses strong *in vitro* anti-inflammatory activity.

2.4. HFF-PS-F5 inhibited NF-κB in LPS-induced RAW 264.7 macrophages

The cytosol and nuclear NF-κB levels of LPS-induced RAW 264.7 are shown in Fig. 31. According to the results, LPS significantly active NF-κB, however, HFF-PS-F5 effectively suppressed NF-κB activation in a dose-dependent manner. These results suggested that HFF-PS-F5 suppresses LPS-induced inflammatory in RAW 264.7 cells by inhibiting the expression of pro-inflammatory cytokines and inflammatory proteins via regulating NF-κB pathway.

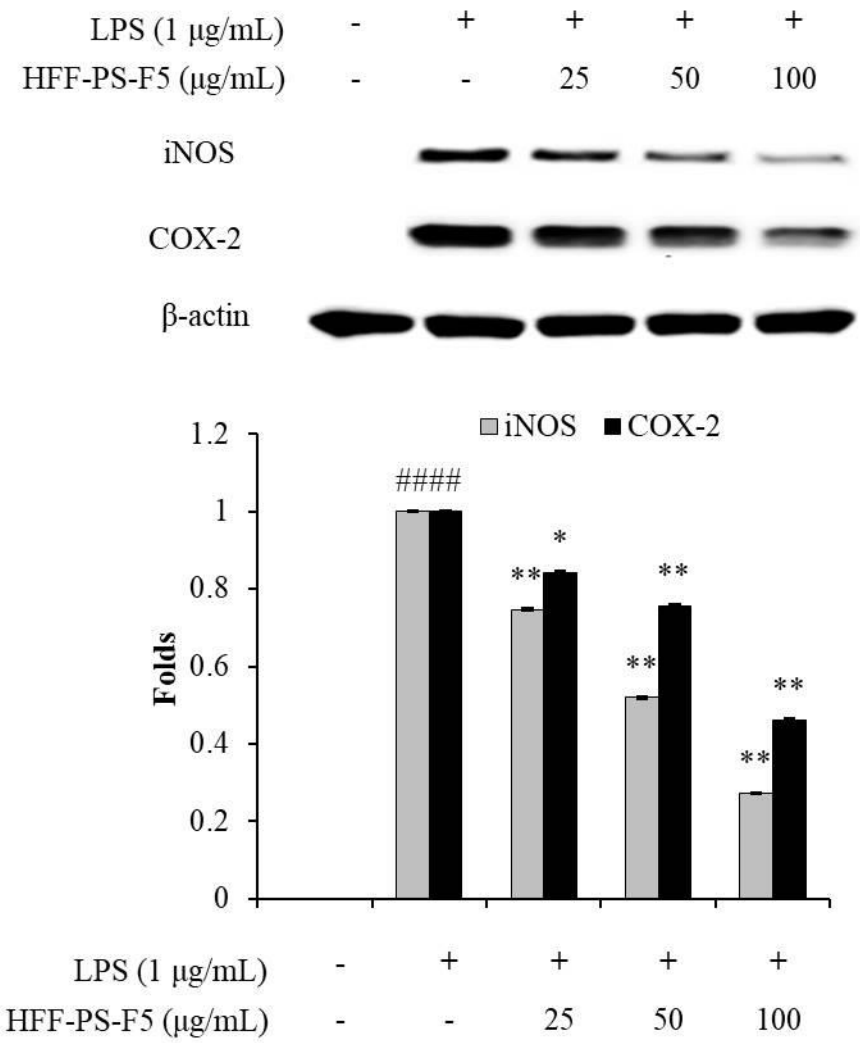

Fig. 30. The inhibitory effect of HFF-PS-F5 on the expression of iNOS and COX-2 proteins in RAW 264.7 macrophages stimulated with LPS. The relative amounts of iNOS and COX-2 levels were compared with β-actin. The experiments were conducted in triplicate, and the data are expressed as the mean ± SE. *$p < 0.05$, ** $p < 0.01$ as compared to the LPS-treated group and $^{\#\#}p < 0.01$ as compared to the control group.

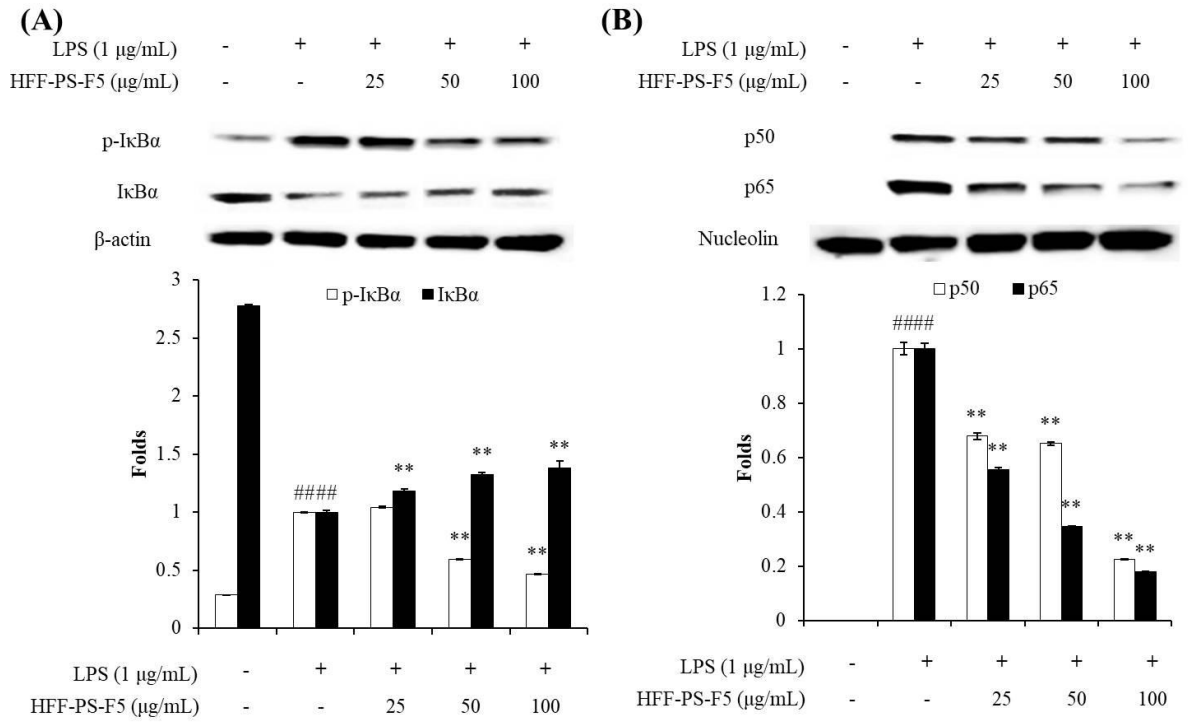

Fig. 31. The inhibitory effect of HFF-PS-F5 on NF-κB activation in RAW 264.7 macrophages stimulated with LPS. (A) The cytosol IκBα and p-IκBα level; (B) the nuclear p50 and p65 NF-κB level. The relative amounts of IκBα and p-IκBα levels were compared with β-actin, and the relative amounts of p50 and p65 NF-κB levels were compared with nucleolin. The experiments were conducted in triplicate, and the data are expressed as the mean ± SE. ** $p < 0.01$ as compared to the LPS-treated group and $^{\#\#}p < 0.01$ as compared to the control group.

2.5. HFF-PS-F4 improved survival rate and reduced heart-beating rate in LPS-induced zebrafish

In vivo evaluation for anti-inflammation activity of SPEH was adopted in zebrafish due to its advantages such as similarity to mammals, short life span, the ability of the female fish to produce a large number of eggs [83, 84]. The survival rates and heart-beating rates of zebrafish were determined. The survival rate and heart-beating rate of zebrafish that did not receive LPS treatment were considered to be 100% (Fig. 32). The survival rate of LPS-treated zebrafish was significantly decreased (Fig. 32A). However, the survival rates of zebrafish pre-treated with HFF-PS-F4 prior to LPS treatment significantly increased. The heart-beating rate of the zebrafish treated with LPS was significantly increased compared to control, but significantly decreased with HFF-PS-F4 treatment.

2.6. Protective effect of HFF-PS-F4 against LPS-induced ROS generation, cell death, and NO production in zebrafish

In the present study, we observed the ROS generation, cell death, and NO generation in zebrafish. The ROS generation and cell death levels of HFF-PS-F4-treated zebrafish were dose-dependently reduced comparing to the zebrafish treated with LPS only (Fig. 33 and 34). Furthermore, HFF-PS-F4 significantly reduced NO production in LPS-stimulated zebrafish (Fig. 35). These results indicated HFF-PS-F4 possess strong *in vivo* anti-inflammatory activity.

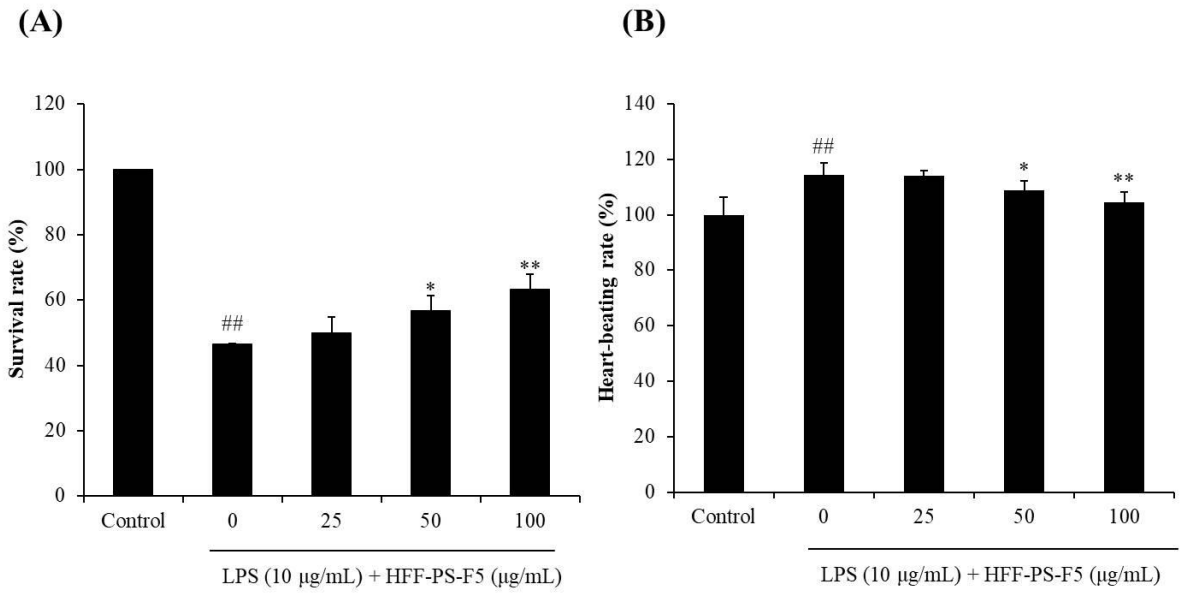

Fig. 32. The survival rate and heart-beating rate of zebrafish after pretreatment with HFF-PS-F5 and/or treatment with LPS. (A) Survival rate; (B) heart-beating rate. The experiments were conducted in triplicate, and the data are expressed as the mean ± SE. *p < 0.05, ** p < 0.01 as compared to the LPS-treated group and $^{\#\#}p$ < 0.01 as compared to the control group.

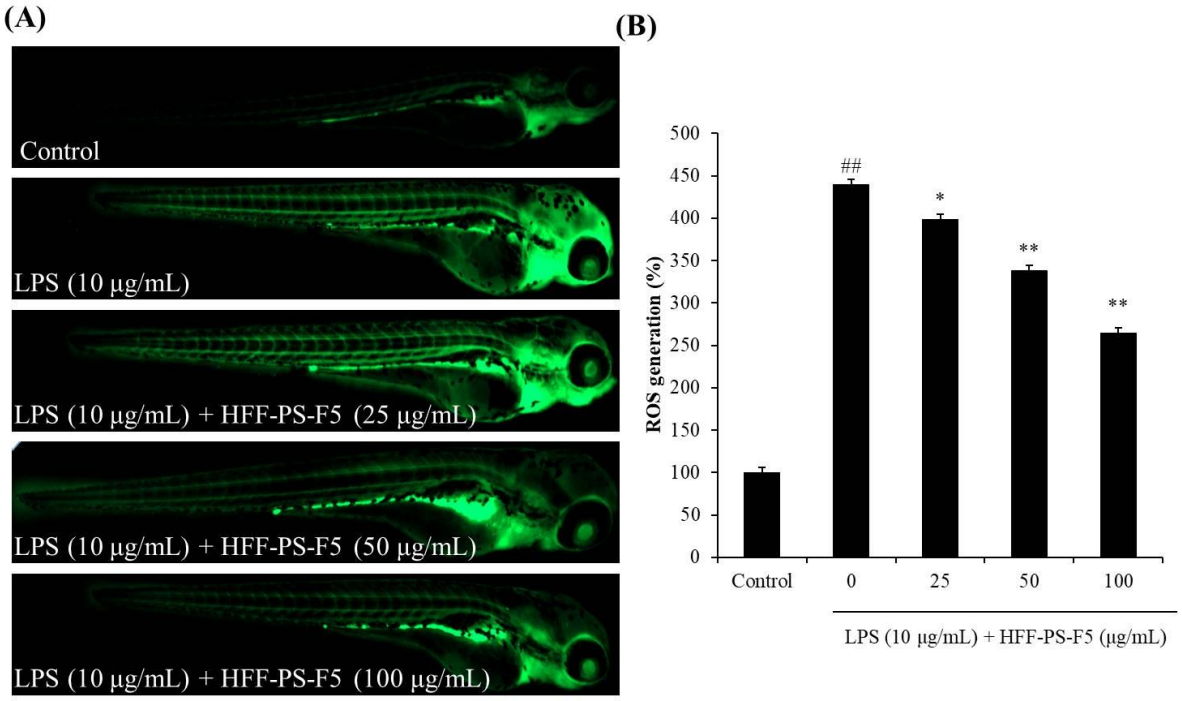

Fig. 33. The protective effect of HFF-PS-F5 during LPS-induced ROS production in zebrafish embryos. (A) Zebrafish embryo under fluorescence microscope; (B) the levels of ROS generation. ROS levels were measured using Image J software. The experiments were conducted in triplicate, and the data are expressed as the mean ± SE. *$p < 0.05$, ** $p < 0.01$ as compared to the LPS-treated group and $^{\#\#}p < 0.01$ as compared to the control group.

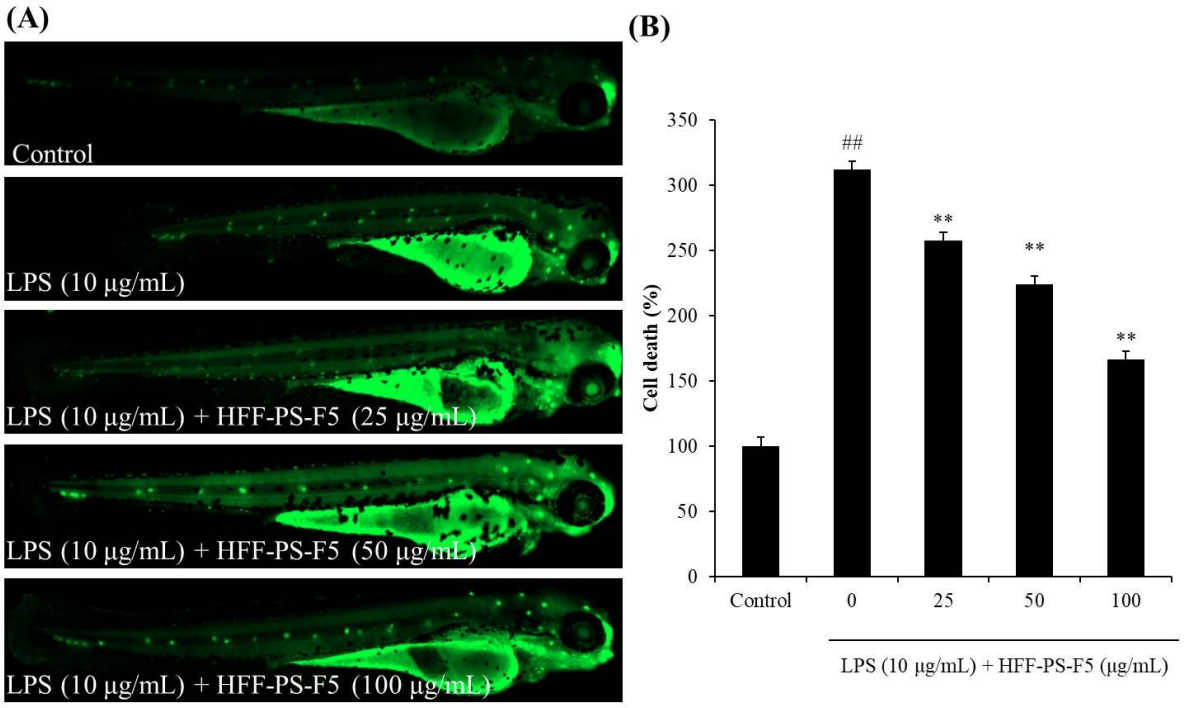

Fig. 34. The protective effect of HFF-PS-F5 during LPS-induced cell death in zebrafish embryos. (A) Zebrafish embryo under fluorescence microscope; (B) the measured levels of cell death. Cell death levels were measured using Image J software. The experiments were conducted in triplicate, and the data are expressed as the mean ± SE. ** $p < 0.01$ as compared to the LPS-treated group and $^{\#\#}p < 0.01$ as compared to the control group.

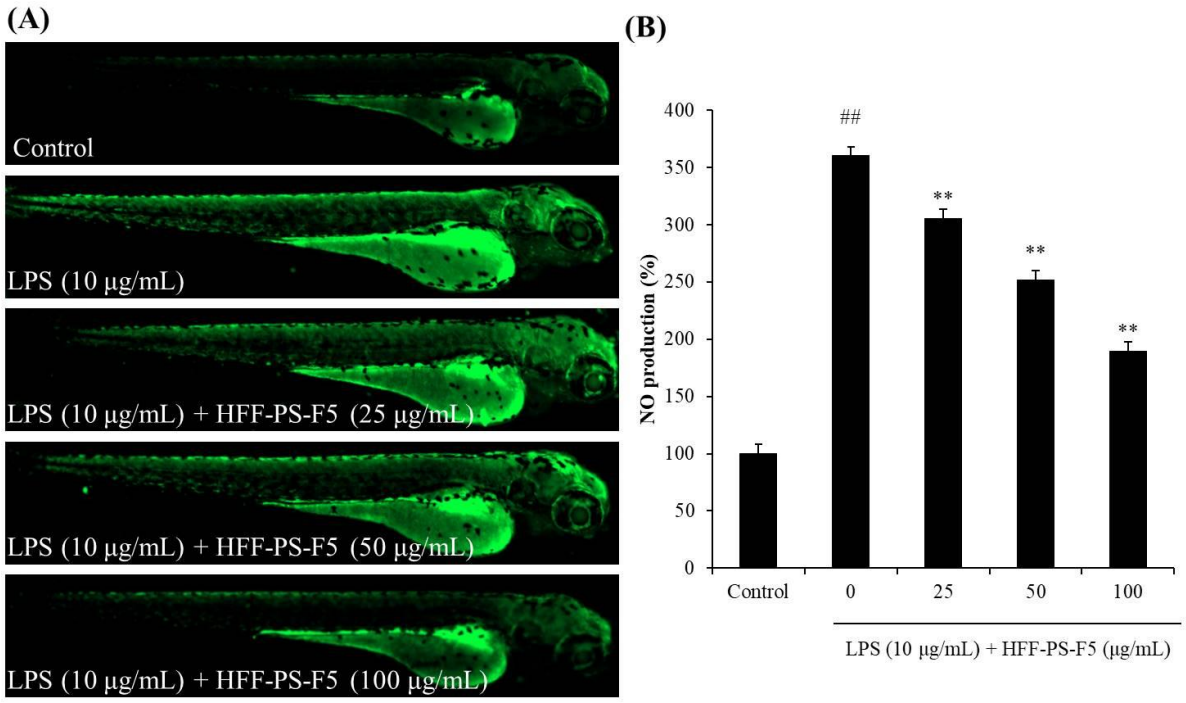

Fig. 35. The effect of HFF-PS-F5 during LPS-induced NO production in zebrafish embryos. (A) Zebrafish embryo under fluorescence microscope; (B) the measured levels of cell death. NO production levels were measured using Image J software. The experiments were conducted in triplicate, and the data are expressed as the mean ± SE. ** $p < 0.01$ as compared to the LPS-treated group and $^{\#\#}p < 0.01$ as compared to the control group.

3. Summary

In summary, HFF-PS-F5 possesses strong *in vitro* anti-inflammatory activity demonstrate in reducing inflammatory molecules production and improving cell viability in LPS-stimulated RAW 264.7 cells. In addition, it possesses strong *in vivo* inflammatory activity demonstrated in improving the survival rate, decreasing heart-beating rate, and reducing ROS and NO generation and cell death in LPS-stimulated zebrafish. The results indicate that HFF-PS-F5 possesses strong *in vitro* and *in vivo* anti-inflammatory activities and could use for developing novel anti-inflammatory drugs or ingredients in cosmetic products.

CONCLUSION

The above results suggested that CA-processing could effective remove the As in *H. fusiforme*. The As could be further removed by fermentation and the bioactivities of *H. fusiforme* could be improved by fermentation. In addition, a fucoidan (HFF-PS-F5) with with an average molecular weight as 213.33 kDa has been isolated from fermented *H. fusiforme* and its bioactivities has been investigated. The results suggest that HFF-PS-F5 may use as a beneficial antioxidant ingredient in medical and cosmetic industries.

REFERENCES

1. Fernando, I.P.S., K.K.A. Sanjeewa, K.W. Samarakoon, W.W. Lee, H.-S. Kim, E.-A. Kim, U.K.D.S.S. Gunasekara, D.T.U. Abeytunga, C. Nanayakkara, E.D. de Silva, H.-S. Lee and Y.-J. Jeon, *FTIR characterization and antioxidant activity of water soluble crude polysaccharides of Sri Lankan marine algae.* ALGAE, 2017. **32**(1): p. 75-86.
2. Kim, H.-H., H.-S. Kim, J.-Y. Ko, C.-Y. Kim, J.-H. Lee and Y.-J. Jeon, *A single-step isolation of useful antioxidant compounds from Ishige okamurae by using centrifugal partition chromatography.* Fisheries and Aquatic Sciences, 2016. **19**(1): p. 22.
3. Kang, N., S.-Y. Kim, S. Rho, J.-Y. Ko and Y.-J. Jeon, *Anti-fatigue activity of a mixture of seahorse (Hippocampus abdominalis) hydrolysate and red ginseng.* Fisheries and Aquatic Sciences, 2017. **20**(1): p. 3.
4. Sanjeewa, K.K.A., I.P.S. Fernando, K.W. Samarakoon, H.H.C. Lakmal, E.-A. Kim, O.N. Kwon, M.G. Dilshara, J.-B. Lee and Y.-J. Jeon, *Anti-inflammatory and anti-cancer activities of sterol rich fraction of cultured marine microalga Nannochloropsis oculata.* ALGAE, 2016. **31**(3): p. 277-287.
5. Fernando, I.P.S., H.-S. Kim, K.K.A. Sanjeewa, J.-Y. Oh, Y.-J. Jeon and W.W. Lee, *Inhibition of inflammatory responses elicited by urban fine dust particles in keratinocytes and macrophages by diphlorethohydroxycarmalol isolated from a brown alga Ishige okamurae.* ALGAE, 2017. **32**(3): p. 261-273.
6. Wang, L., M.-J. Jo, R. Katagiri, K. Harata, M. Ohta, A. Ogawa, M. Kamegai, Y. Ishida, S. Tanoue, S. Kimura, S.-C. Lee and Y.-J. Jeon, *Antioxidant effects of citrus pomace extracts processed by super-heated steam.* LWT, 2018. **90**: p. 331-338.

7. Shanura, F.I.P., K. Misook, S. Kwang-Tae, J. Yoonhwa and J. You-Jin, *Antioxidant Activity of Marine Algal Polyphenolic Compounds: A Mechanistic Approach.* 2016. **19**(7): p. 615-628.

8. Kim, Y.-S., J.-W. Hwang, S.-H. Sung, Y.-J. Jeon, J.-H. Jeong, B.-T. Jeon, S.-H. Moon and P.-J. Park, *Antioxidant activity and protective effect of extract of Celosia cristata L. flower on tert-butyl hydroperoxide-induced oxidative hepatotoxicity.* Food Chemistry, 2015. **168**: p. 572-579.

9. Heo, S.-J., W.-J. Yoon, K.-N. Kim, G.-N. Ahn, S.-M. Kang, D.-H. Kang, A. affan, C. Oh, W.-K. Jung and Y.-J. Jeon, *Evaluation of anti-inflammatory effect of fucoxanthin isolated from brown algae in lipopolysaccharide-stimulated RAW 264.7 macrophages.* Food and Chemical Toxicology, 2010. **48**(8): p. 2045-2051.

10. Frostegård, J., A.-K. Ulfgren, P. Nyberg, U. Hedin, J. Swedenborg, U. Andersson and G.K. Hansson, *Cytokine expression in advanced human atherosclerotic plaques: dominance of pro-inflammatory (Th1) and macrophage-stimulating cytokines.* Atherosclerosis, 1999. **145**(1): p. 33-43.

11. Sanjeewa, K.K.A., I.P.S. Fernando, S.-Y. Kim, W.-S. Kim, G. Ahn, Y. Jee and Y.-J. Jeon, *Ecklonia cava (Laminariales) and Sargassum horneri (Fucales) synergistically inhibit the lipopolysaccharide-induced inflammation via blocking NF-κB and MAPK pathways.* ALGAE, 2019. **34**(1): p. 45-56.

12. Sanjeewa, K.K.A., T.U. Jayawardena, H.-S. Kim, S.-Y. Kim, G. Ahn, H.-J. Kim, X. Fu, Y. Jee and Y.-J. Jeon, *Ethanol extract separated from Sargassum horneri (Turner) abate LPS-induced inflammation in RAW 264.7 macrophages.* Fisheries and Aquatic Sciences, 2019. **22**(1): p. 6.

13. Lee, H.J., E.-A. Hyun, W.J. Yoon, B.H. Kim, M.H. Rhee, H.K. Kang, J.Y. Cho and E.S. Yoo, *In vitro anti-inflammatory and anti-oxidative effects of Cinnamomum camphora extracts.* Journal of Ethnopharmacology, 2006. **103**(2): p. 208-216.

14. Heo, S.-J., E.-J. Park, K.-W. Lee and Y.-J. Jeon, *Antioxidant activities of enzymatic extracts from brown seaweeds.* Bioresource Technology, 2005. **96**(14): p. 1613-1623.

15. Nguyen, V.-T., S.-C. Ko, S.-J. Heo, D.-H. Kang, C. Oh, K.-N. Kim, Y.-J. Jeon, Y.-M. Kim, W.S. Park, I.-W. Choi, N.G. Park and W.-K. Jung, *Ciona intestinalis calcitonin-like peptide promotes osteoblast differentiation and mineralization through MAPK pathway in MC3T3-E1 cells.* Process Biochemistry, 2018. **67**: p. 127-138.

16. Fernando, I.P.S., K.K.A. Sanjeewa, Y.-S. Ann, C.-i. Ko, S.-H. Lee, W.W. Lee and Y.-J. Jeon, *Apoptotic and antiproliferative effects of Stigmast-5-en-3-ol from Dendronephthya gigantea on human leukemia HL-60 and human breast cancer MCF-7 cells.* Toxicology in Vitro, 2018. **52**: p. 297-305.

17. Park, C., J.-W. Jeong, D.-S. Lee, M.-J. Yim, J. Lee, M. Han, S. Kim, H.-S. Kim, G.-Y. Kim, E. Park, Y.-J. Jeon, H.-J. Cha and Y. Choi, *Sargassum serratifolium Extract Attenuates Interleukin-1β-Induced Oxidative Stress and Inflammatory Response in Chondrocytes by Suppressing the Activation of NF-κB, p38 MAPK, and PI3K/Akt.* International Journal of Molecular Sciences, 2018. **19**(8): p. 2308.

18. Fernando, I.P.S., K.K.A. Sanjeewa, H.-S. Kim, L. Wang, W.W. Lee and Y.-J. Jeon, *Apoptotic and antiproliferative properties of 3β-hydroxy-Δ5-steroidal congeners from a partially purified column fraction of Dendronephthya gigantea against HL-60 and MCF-7 cancer cells.* Journal of Applied Toxicology, 2018. **38**(4): p. 527-536.

19. Kumaresan, M., K. Vijai Anand, K. Govindaraju, S. Tamilselvan and V. Ganesh Kumar, *Seaweed Sargassum wightii mediated preparation of zirconia (ZrO2)*

nanoparticles and their antibacterial activity against gram positive and gram negative bacteria. Microbial Pathogenesis, 2018. **124**: p. 311-315.

20. Praiboon, J., S. Palakas, T. Noiraksa and K. Miyashita, *Seasonal variation in nutritional composition and anti-proliferative activity of brown seaweed, Sargassum oligocystum.* J Appl Physiol, 2018. **30**(1): p. 101-111.

21. Ahn, C.-B., Y.-J. Jeon, Y.-T. Kim and J.-Y. Je, *Angiotensin I converting enzyme (ACE) inhibitory peptides from salmon byproduct protein hydrolysate by Alcalase hydrolysis.* Process Biochemistry, 2012. **47**(12): p. 2240-2245.

22. Kang, M.-C., N. Kang, S.-C. Ko, Y.-B. Kim and Y.-J. Jeon, *Anti-obesity effects of seaweeds of Jeju Island on the differentiation of 3T3-L1 preadipocytes and obese mice fed a high-fat diet.* Food and Chemical Toxicology, 2016. **90**: p. 36-44.

23. Sun, H.-H., W.-J. Mao, Y. Chen, S.-D. Guo, H.-Y. Li, X.-H. Qi, Y.-L. Chen and J. Xu, *Isolation, chemical characteristics and antioxidant properties of the polysaccharides from marine fungus Penicillium sp. F23-2.* Carbohyd Polym, 2009. **78**(1): p. 117-124.

24. Ko, S.-C., J.-K. Lee, H.-G. Byun, S.-C. Lee and Y.-J. Jeon, *Purification and characterization of angiotensin I-converting enzyme inhibitory peptide from enzymatic hydrolysates of Styela clava flesh tissue.* Process Biochemistry, 2012. **47**(1): p. 34-40.

25. Wang, L., Y.-J. Park, Y.-J. Jeon and B. Ryu, *Bioactivities of the edible brown seaweed, Undaria pinnatifida: A review.* Aquaculture, 2018. **495**: p. 873-880.

26. Sun, Z., Z. Dai, W. Zhang, S. Fan, H. Liu, R. Liu and T. Zhao, *12 - Antiobesity, Antidiabetic, Antioxidative, and Antihyperlipidemic Activities of Bioactive Seaweed Substances*, in *Bioactive Seaweeds for Food Applications*, Y. Qin, Editor. 2018, Academic Press. p. 239-253.

27. Ferreira, J., A.A. Ramos, T. Almeida, A. Azqueta and E. Rocha, *Drug resistance in glioblastoma and cytotoxicity of seaweed compounds, alone and in combination with anticancer drugs: A mini review.* Phytomedicine, 2018. **48**: p. 84-93.

28. Sanjeewa, K.K.A., N. Kang, G. Ahn, Y. Jee, Y.-T. Kim and Y.-J. Jeon, *Bioactive potentials of sulfated polysaccharides isolated from brown seaweed Sargassum spp in related to human health applications: A review.* Food Hydrocolloids, 2018. **81**: p. 200-208.

29. Fernando, I.P.S., D. Kim, J.-W. Nah and Y.-J. Jeon, *Advances in functionalizing fucoidans and alginates (bio)polymers by structural modifications: A review.* Chemical Engineering Journal, 2019. **355**: p. 33-48.

30. Shanura Fernando, I.P., K.K. Asanka Sanjeewa, K.W. Samarakoon, H.-S. Kim, U.K.D.S.S. Gunasekara, Y.-J. Park, D.T.U. Abeytunga, W.W. Lee and Y.-J. Jeon, *The potential of fucoidans from Chnoospora minima and Sargassum polycystum in cosmetics: antioxidant, anti-inflammatory, skin-whitening, and antiwrinkle activities.* J Appl Physiol, 2018.

31. Fernando, I.P.S., K.K.A. Sanjeewa, S.-Y. Kim, J.-S. Lee and Y.-J. Jeon, *Reduction of heavy metal (Pb2+) biosorption in zebrafish model using alginic acid purified from Ecklonia cava and two of its synthetic derivatives.* International Journal of Biological Macromolecules, 2018. **106**: p. 330-337.

32. Fernando, I.P.S., T.U. Jayawardena, K.K.A. Sanjeewa, L. Wang, Y.-J. Jeon and W.W. Lee, *Anti-inflammatory potential of alginic acid from Sargassum horneri against urban aerosol-induced inflammatory responses in keratinocytes and macrophages.* Ecotoxicology and Environmental Safety, 2018. **160**: p. 24-31.

33. Asanka Sanjeewa, K.K., W.W. Lee, J.-I. Kim and Y.-J. Jeon, *Exploiting biological activities of brown seaweed Ishige okamurae Yendo for potential industrial applications: a review.* Journal of Applied Phycology, 2017. **29**(6): p. 3109-3119.

34. Lee, J.-H., J.-Y. Ko, E.-A. Kim, E.-K. Hwang, C.S. Park, J.-S. Lee, C.-Y. Kim, H.-S. Lee, H.-K. Kang, S.-H. Cha and Y.-J. Jeon, *Identification and large isolation of an anti-inflammatory compound from an edible brown seaweed, Undariopsis peterseniana, and evaluation on its anti-inflammatory effect in in vitro and in vivo zebrafish.* J Appl Physiol, 2017. **29**(3): p. 1587-1596.

35. De Souza, É.T., D. Pereira de Lira, A. Cavalcanti de Queiroz, D.J. Costa da Silva, A. Bezerra de Aquino, E. Campessato Mella, V. Prates Lorenzo, G.E. De Miranda, J.X. De Araújo-Júnior, M.C. De Oliveira Chaves, J.M. Barbosa-Filho, P. Filgueiras de Athayde-Filho, B.V. De Oliveira Santos and M.S. Alexandre-Moreira, *The Antinociceptive and Anti-Inflammatory Activities of Caulerpin, a Bisindole Alkaloid Isolated from Seaweeds of the Genus Caulerpa.* Marine Drugs, 2009. **7**(4): p. 689.

36. Wijesinghe, W.A.J.P., Y. Athukorala and Y.-J. Jeon, *Effect of anticoagulative sulfated polysaccharide purified from enzyme-assistant extract of a brown seaweed Ecklonia cava on Wistar rats.* Carbohyd Polym, 2011. **86**(2): p. 917-921.

37. Heo, S.-J. and Y.-J. Jeon, *Protective effect of fucoxanthin isolated from Sargassum siliquastrum on UV-B induced cell damage.* Journal of Photochemistry and Photobiology B: Biology, 2009. **95**(2): p. 101-107.

38. Kang, M.-C., G. Ahn, X. Yang, K.-N. Kim, S.-M. Kang, S.-H. Lee, S.-C. Ko, J.-Y. Ko, D. Kim, Y.-T. Kim, Y. Jee, S.-J. Park and Y.-J. Jeon, *Hepatoprotective effects of dieckol-rich phlorotannins from Ecklonia cava, a brown seaweed, against ethanol*

induced liver damage in BALB/c mice. Food Chem Toxicol, 2012. **50**(6): p. 1986-1991.

39. Wang, L., Y.R. Cui, H.-W. Yang, H.G. Lee, J.-Y. Ko and Y.-J. Jeon, *A mixture of seaweed extracts and glycosaminoglycans from sea squirts inhibits α-MSH-induced melanogenesis in B16F10 melanoma cells.* Fisheries and Aquatic Sciences, 2019. **22**(1): p. 11.

40. Hou, X. and X. Yan, *Study on the concentration and seasonal variation of inorganic elements in 35 species of marine algae.* Science of The Total Environment, 1998. **222**(3): p. 141-156.

41. Romarís-Hortas, V., A. Moreda-Piñeiro and P. Bermejo-Barrera, *Microwave assisted extraction of iodine and bromine from edible seaweed for inductively coupled plasma-mass spectrometry determination.* Talanta, 2009. **79**(3): p. 947-952.

42. Kumar, K.S., K. Ganesan and P.V.S. Rao, *Antioxidant potential of solvent extracts of Kappaphycus alvarezii (Doty) Doty – An edible seaweed.* Food Chemistry, 2008. **107**(1): p. 289-295.

43. Zhao, Y., J. Wu, D. Shang, J. Ning, Y. Zhai, X. Sheng and H. Ding, *Subcellular distribution and chemical forms of cadmium in the edible seaweed, Porphyra yezoensis.* Food Chemistry, 2015. **168**: p. 48-54.

44. Sundbæk, K.B., I.D.W. Koch, C.G. Villaro, N.S. Rasmussen, S.L. Holdt and N.B. Hartmann, *Sorption of fluorescent polystyrene microplastic particles to edible seaweed Fucus vesiculosus.* J Appl Physiol, 2018.

45. Liu, D., J.K. Keesing, Z. Dong, Y. Zhen, B. Di, Y. Shi, P. Fearns and P. Shi, *Recurrence of the world's largest green-tide in 2009 in Yellow Sea, China: Porphyra*

yezoensis aquaculture rafts confirmed as nursery for macroalgal blooms. Marine Pollution Bulletin, 2010. **60**(9): p. 1423-1432.

46. Hay, C.H. and P.A. Luckens, *The Asian kelp Undaria pinnatifida (Phaeophyta: Laminariales) found in a New Zealand harbour*. New Zealand Journal of Botany, 1987. **25**(2): p. 329-332.

47. Wang, L., J.Y. Oh, H.S. Kim, W. Lee, Y. Cui, H.G. Lee, Y.-T. Kim, J.Y. Ko and Y.-J. Jeon, *Protective effect of polysaccharides from Celluclast-assisted extract of Hizikia fusiforme against hydrogen peroxide-induced oxidative stress in vitro in Vero cells and in vivo in zebrafish.* International Journal of Biological Macromolecules, 2018. **112**: p. 483-489.

48. Fernandes, F., M. Barbosa, D.M. Pereira, I. Sousa-Pinto, P. Valentão, I.C. Azevedo and P.B. Andrade, *Chemical profiling of edible seaweed (Ochrophyta) extracts and assessment of their in vitro effects on cell-free enzyme systems and on the viability of glutamate-injured SH-SY5Y cells.* Food Chem Toxicol, 2018. **116**: p. 196-206.

49. Wang, L., J.Y. Oh, J. Hwang, J.Y. Ko, Y.-J. Jeon and B. Ryu, *In Vitro and In Vivo Antioxidant Activities of Polysaccharides Isolated from Celluclast-Assisted Extract of an Edible Brown Seaweed, Sargassum fulvellum.* Antioxidants, 2019. **8**(10): p. 493.

50. Ngo, D.-H. and S.-K. Kim, *Sulfated polysaccharides as bioactive agents from marine algae.* International Journal of Biological Macromolecules, 2013. **62**: p. 70-75.

51. Wang, L., W. Lee, J.Y. Oh, Y.R. Cui, B. Ryu and Y.-J. Jeon, *Protective Effect of Sulfated Polysaccharides from Celluclast-Assisted Extract of Hizikia fusiforme Against Ultraviolet B-Induced Skin Damage by Regulating NF-κB, AP-1, and MAPKs Signaling Pathways In Vitro in Human Dermal Fibroblasts.* 2018. **16**(7): p. 239-247.

52. Sanjeewa, K.K.A., I.P.S. Fernando, S.-Y. Kim, H.-S. Kim, G. Ahn, Y. Jee and Y.-J. Jeon, *In vitro and in vivo anti-inflammatory activities of high molecular weight sulfated polysaccharide; containing fucose separated from Sargassum horneri: Short communication.* International Journal of Biological Macromolecules, 2018. **107**: p. 803-807.

53. Wijesekara, I., R. Pangestuti and S.-K. Kim, *Biological activities and potential health benefits of sulfated polysaccharides derived from marine algae.* Carbohydrate Polymers, 2011. **84**(1): p. 14-21.

54. Hu, L., J. Tan, X. Yang, H. Tan, X. Xu, M. You, W. Qin, L. Huang, S. Li, M. Mo, H. Wei, J. Li and J. Tan, *Polysaccharide Extracted from Laminaria japonica Delays Intrinsic Skin Aging in Mice.* Evidence-Based Complementary and Alternative Medicine, 2016. **2016**: p. 8.

55. Hwang, P.-A., S.-Y. Chien, Y.-L. Chan, M.-K. Lu, C.-H. Wu, Z.-L. Kong and C.-J. Wu, *Inhibition of Lipopolysaccharide (LPS)-Induced Inflammatory Responses by Sargassum hemiphyllum Sulfated Polysaccharide Extract in RAW 264.7 Macrophage Cells.* Journal of Agricultural and Food Chemistry, 2011. **59**(5): p. 2062-2068.

56. Pratoomthai, B., T. Songtavisin, W. Gangnonngiw and K. Wongprasert, *In vitro inhibitory effect of sulfated galactans isolated from red alga Gracilaria fisheri on melanogenesis in B16F10 melanoma cells.* Journal of Applied Phycology, 2018. **30**(4): p. 2611-2618.

57. Wang, L., W. Lee, J. Oh, Y. Cui, B. Ryu and Y.-J. Jeon, *Protective Effect of Sulfated Polysaccharides from Celluclast-Assisted Extract of Hizikia fusiforme Against Ultraviolet B-Induced Skin Damage by Regulating NF-κB, AP-1, and MAPKs*

Signaling Pathways In Vitro in Human Dermal Fibroblasts. Marine Drugs, 2018. **16**(7): p. 239.

58. Wang, L., W. Lee, J.Y. Oh, Y.R. Cui, B. Ryu and Y.-J. Jeon, *Protective Effect of Sulfated Polysaccharides from Celluclast-Assisted Extract of Hizikia fusiforme Against Ultraviolet B-Induced Skin Damage by Regulating NF-κB, AP-1, and MAPKs Signaling Pathways In Vitro in Human Dermal Fibroblasts.* Marine Drugs, 2018. **16**(7): p. 239.

59. Wang, L., J.Y. Oh, T.U. Jayawardena, Y.-J. Jeon and B. Ryu, *Anti-inflammatory and anti-melanogenesis activities of sulfated polysaccharides isolated from Hizikia fusiforme: Short communication.* International Journal of Biological Macromolecules, 2019.

60. Wang, L., J.Y. Oh, H.-W. Yang, H.S. Kim and Y.-J. Jeon, *Protective effect of sulfated polysaccharides from a Celluclast-assisted extract of Hizikia fusiforme against ultraviolet B-induced photoaging in vitro in human keratinocytes and in vivo in zebrafish.* Marine Life Science & Technology, 2019.

61. Sayago, A., R. Beltrán, M.A.F. Recamales and J.L. Gómez-Ariza, *Optimization of an HPLC-HG-AFS method for screening Sb(v), Sb(iii), and Me3SbBr2 in water samples.* Journal of Analytical Atomic Spectrometry, 2002. **17**(10): p. 1400-1404.

62. Nash, M.J., J.E. Maskall and S.J. Hill, *Developments with anion exchange stationary phases for HPLC-ICP-MS analysis of antimony species.* Analyst, 2006. **131**(6): p. 724-730.

63. Sánchez-Rodas, D., W.T. Corns, B. Chen and P.B. Stockwell, *Atomic Fluorescence Spectrometry: a suitable detection technique in speciation studies for arsenic,*

selenium, antimony and mercury. Journal of Analytical Atomic Spectrometry, 2010. **25**(7): p. 933-946.

64. Yu, Y., L. Wang, X. Fu, L. Wang, X. Fu, M. Yang, Z. Han, H. Mou and Y.-J. Jeon, *Anti-oxidant and anti-inflammatory activities of ultrasonic-assistant extracted polyphenol-rich compounds from Sargassum muticum.* Journal of Oceanology and Limnology, 2019. **37**(3): p. 836-847.

65. Omidkhoda, A., H. Mozdarani, A. Movasaghpoor and A.A.P. Fatholah, *Study of apoptosis in labeled mesenchymal stem cells with superparamagnetic iron oxide using neutral comet assay.* Toxicology in Vitro, 2007. **21**(6): p. 1191-1196.

66. Robin, M.B., *The Color and Electronic Configurations of Prussian Blue.* Inorganic Chemistry, 1962. **1**(2): p. 337-342.

67. Chemists, A.o.O.A., *Official methods of analysis of the Association of Official Analytical Chemists*. Vol. 1. 1990: The Association.

68. Kang, S.-M., K.-N. Kim, S.-H. Lee, G. Ahn, S.-H. Cha, A.-D. Kim, X.-D. Yang, M.-C. Kang and Y.-J. Jeon, *Anti-inflammatory activity of polysaccharide purified from AMG-assistant extract of Ecklonia cava in LPS-stimulated RAW 264.7 macrophages.* Carbohydrate Polymers, 2011. **85**(1): p. 80-85.

69. Jayawardena, T.U., I.P.S. Fernando, W.W. Lee, K.K.A. Sanjeewa, H.-S. Kim, D.-S. Lee and Y.-J. Jeon, *Isolation and purification of fucoidan fraction in Turbinaria ornata from the Maldives; Inflammation inhibitory potential under LPS stimulated conditions in in-vitro and in-vivo models.* International Journal of Biological Macromolecules, 2019. **131**: p. 614-623.

70. Raguraman, V., S.A. L, J. J, S. Palaniappan, S. Gopal, T. R and K. R, *Sulfated polysaccharide from Sargassum tenerrimum attenuates oxidative stress induced*

reactive oxygen species production in in vitro and in zebrafish model. Carbohydrate Polymers, 2019. **203**: p. 441-449.

71. Wang, L., B. Ryu, W.-S. Kim, G.H. Kim and Y.-J. Jeon, *Protective effect of gallic acid derivatives from the freshwater green alga <italic>Spirogyra</italic> sp. against ultraviolet B-induced apoptosis through reactive oxygen species clearance in human keratinocytes and zebrafish.* Algae, 2017. **32**(4): p. 379-388.

72. Wijesinghe, W.A.J.P., Y.J. Jeon, P. Ramasamy, M.E.A. Wahid and C.S. Vairappan, *Anticancer activity and mediation of apoptosis in human HL-60 leukaemia cells by edible sea cucumber (Holothuria edulis) extract.* Food Chemistry, 2013. **139**(1): p. 326-331.

73. Kang, M.-C., S.-Y. Kim, E.-A. Kim, J.-H. Lee, Y.-S. Kim, S.-K. Yu, J.B. Chae, I.-H. Choe, J.H. Cho and Y.-J. Jeon, *Antioxidant activity of polysaccharide purified from Acanthopanax koreanum Nakai stems in vitro and in vivo zebrafish model.* Carbohydrate Polymers, 2015. **127**: p. 38-46.

74. Baird, L. and A.T. Dinkova-Kostova, *The cytoprotective role of the Keap1–Nrf2 pathway.* Archives of Toxicology, 2011. **85**(4): p. 241-272.

75. Loboda, A., M. Damulewicz, E. Pyza, A. Jozkowicz and J. Dulak, *Role of Nrf2/HO-1 system in development, oxidative stress response and diseases: an evolutionarily conserved mechanism.* Cellular and Molecular Life Sciences, 2016. **73**(17): p. 3221-3247.

76. Kim, S.-Y., E.-A. Kim, Y.-S. Kim, S.-K. Yu, C. Choi, J.-S. Lee, Y.-T. Kim, J.-W. Nah and Y.-J. Jeon, *Protective effects of polysaccharides from Psidium guajava leaves against oxidative stresses.* International Journal of Biological Macromolecules, 2016. **91**: p. 804-811.

77. Lee, S.-H., C.-I. Ko, Y. Jee, Y. Jeong, M. Kim, J.-S. Kim and Y.-J. Jeon, *Anti-inflammatory effect of fucoidan extracted from Ecklonia cava in zebrafish model.* Carbohyd Polym, 2013. **92**(1): p. 84-89.

78. Kim, K.-N., Y.-J. Ko, H.-M. Yang, Y.-M. Ham, S.W. Roh, Y.-J. Jeon, G. Ahn, M.-C. Kang, W.-J. Yoon, D. Kim and T. Oda, *Anti-inflammatory effect of essential oil and its constituents from fingered citron (Citrus medica L. var. sarcodactylis) through blocking JNK, ERK and NF-κB signaling pathways in LPS-activated RAW 264.7 cells.* Food Chem Toxicol, 2013. **57**: p. 126-131.

79. Ko, S.-C. and Y.-J. Jeon, *Anti-inflammatory effect of enzymatic hydrolysates from Styela clava flesh tissue in lipopolysaccharide-stimulated RAW 264.7 macrophages and in vivo zebrafish model.* Nutr Res Pract, 2015. **9**(3): p. 219-226.

80. Cheong, S.H., H.-W. Yang, E.-Y. Ko, G. Ahn, W. Lee, D. Kim, Y.-J. Jeon and K.-N. Kim, *Anti-inflammatory effects of trans-1,3-diphenyl-2,3-epoxypropane-1-one in zebrafish embryos in vivo model.* Fish & Shellfish Immunology, 2016. **50**: p. 16-20.

81. Kim, S.F., D.A. Huri and S.H. Snyder, *Inducible nitric oxide synthase binds, S-nitrosylates, and activates cyclooxygenase-2.* Science, 2005. **310**(5756): p. 1966-1970.

82. Xiong, H., Y. Cheng, X. Zhang and X. Zhang, *Effects of taraxasterol on iNOS and COX-2 expression in LPS-induced RAW 264.7 macrophages.* Journal of Ethnopharmacology, 2014. **155**(1): p. 753-757.

83. Kishi, S., J. Uchiyama, A.M. Baughman, T. Goto, M.C. Lin and S.B. Tsai, *The zebrafish as a vertebrate model of functional aging and very gradual senescence.* Experimental Gerontology, 2003. **38**(7): p. 777-786.

84. Ko, S.-C., S.-H. Cha, S.-J. Heo, S.-H. Lee, S.-M. Kang and Y.-J. Jeon, *Protective effect of Ecklonia cava on UVB-induced oxidative stress: in vitro and in vivo zebrafish model.* J Appl Physiol, 2011. **23**(4): p. 697-708.

감사의 글

지난 3 년동안 박사과정을 순조롭게 마무리하도록 많은 관심과 배려,세심한 가르침을 아끼지 않으신 전유진 지도교수님께 진심으로 감사를 드립니다.

부족한 논문의 심사를 맡아 많은 지도와 조언을 해 주신 김기영교수님, 송춘복 교수님과 요재영,류보미박사님께 감사드리고, 저의 대학원 과정 중 많은 도움을 주신 여러 학과 교수님께도 감사 드립니다.

본 박사과정을 수행할수 있도록 여건을 허락하여 주시고 여러가지 지원을 아끼지 않으신 신생활그룹 안봉락회장님, 캉마이천의 장재중사장님, 안봉자부총경리과 모든 임원님들께 진심으로 감사의 고마움을 전합니다.

그리고 이 논문이 완성되기까지 해양생명과학 실험실 王雷박사와 여러 선후배님, 저와 함께 동고동락하면서 온갖 실험과 어려운 일을 마다 하지 않고 곁에서 도와준 캉마이천 식품연구소 吕印文경리,이향경리외 모든 연구원들, 그리고 구조 특성 실험에 결정적인 도움을 주신 중국해양대학 付晓婷부교수님께도 감사드립니다.

이 모든 영광과 결실을 하늘나라에 계시는 아버지、어머니、장인, "우리집안에도 박사가 나왔네"하시면서 기쁨과 눈물을 보이시던 장모님, 희생을 마다 않고 뒷바라지를 해준 아내 노경자 사랑하는 아들 내외와 함께 나누고 싶습니다.

감사합니다.